Heterocyclic 1,3-diazepine-based thiones and selones as versatile halogen bond acceptors

Authors

Arianna C. Ragusa^a, Andrew J. Peloquin^a, Marjan M. Shahani^b, Keri N. Dowling^b, James A. Golen^c, Colin D. McMillen^a, Daniel Rabinovich^{bd} and William T. Pennington^a*

^aDepartment of Chemistry, Clemson University, 219 Hunter Laboratories, Clemson, SC, 29634, USA ^bDepartment of Chemistry, University of North Carolina at Charlotte, 9201 University City Blvd, Charlotte, NC, 28223, USA

^cDepartment of Chemistry and Biochemistry, University of Massachusetts Dartmouth, North Dartmouth, MA, 02747, USA

^d Joint School of Nanoscience and Nanoengineering, 2907 E. Gate City Blvd, Greensboro, NC, 27401, USA

Correspondence email: billp@clemson.edu

Funding information Air Force Institute of Technology (scholarship to Andrew J. Peloquin); National Science Foundation (grant No. CHE-1560300; grant No. CHE-2050042).

Synopsis Utilizing the N-heterocyclic chalcogenones hexahydro-1,3-bis(2,4,6-trimethylphenyl)-2H-1,3-diazepine-2-thione (SDiazMesS) and hexahydro-1,3-bis(2,4,6-trimethylphenyl)-2H-1,3-diazepine-2-selone (SDiazMesSe) as halogen bond acceptors, 24 new cocrystals were prepared. The solid-state structure of the parent molecules was also determined, along with those of their acetonitrile solvates.

Abstract Utilizing the N-heterocyclic chalcogenones hexahydro-1,3-bis(2,4,6-trimethylphenyl)-2H-1,3-diazepine-2-thione (**SDiazMesS**) and hexahydro-1,3-bis(2,4,6-trimethylphenyl)-2H-1,3-diazepine-2-selone (**SDiazMesSe**) as halogen bond acceptors, a total of 24 new cocrystals were prepared. The solid-state structure of the parent molecules was also determined, along with those of their acetonitrile solvates. Through the reaction of the chalcogen atom with molecular diiodine, a variety of S–I–I and Se–I–I fragments were formed, spanning a wide range of I–I bond orders. With acetone as a reaction solvent, molecular diiodine causes the oxidative addition of acetone to the chalcogen atom, resulting in new C–S, C–Se, and C–C covalent bonds under mild conditions. The common halogen bond donors, iodopentafluorobenzene, 1,2-, 1,3-, and 1,4-diiodotetrafluorobenzene,

1,3,5-trifluorotriiodobenzene, and tetraiodoethylene resulted in halogen-bond driven cocrystal formation. In most cases, the analogous SDiazMesS and SDiazMesSe cocrystals were isomorphic.

Keywords: halogen bonding, thione, selone, organoiodine, diiodine

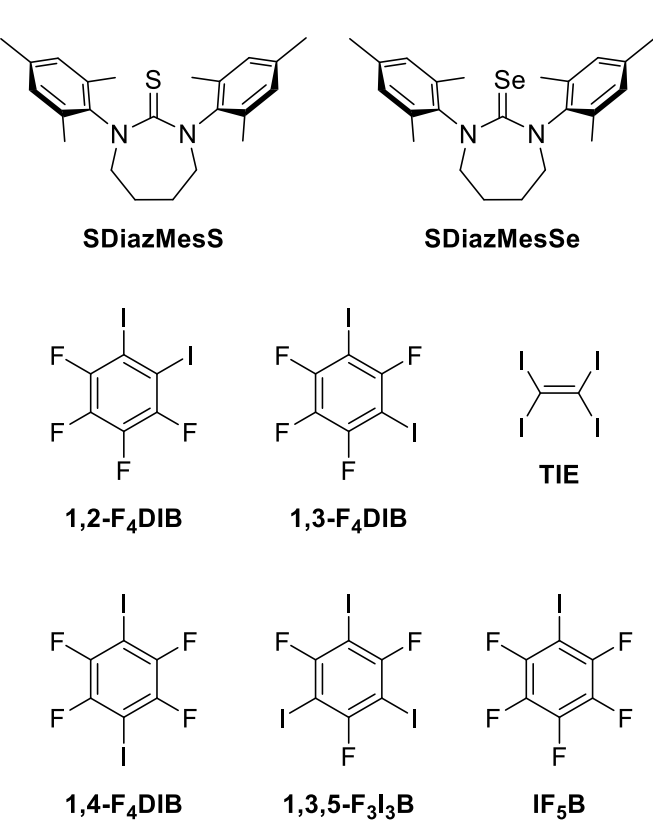
1. Introduction

Halogen bonding has long been known, and formally defined by the International Union of Pure and Applied Chemistry (IUPAC) in 2013, as an attractive interaction between an electrophilic region on a halogen atom (halogen-bond donor) and a nucleophilic region on another atom or molecule (halogen-bond acceptor) (Desiraju *et al.*, 2013). The electrophilic region is referred to as the σ hole and is located at the "cap" on the halogen end of the covalent bond, and is accompanied by a "belt" of relatively higher electrostatic potential orthogonal to the bond (Murray *et al.*, 2009; Politzer *et al.*, 2010; Politzer & Murray, 2017). A similar electron density distribution is observed for the chalcogen atoms and is particularly pronounced for thiones and selones (Vogel *et al.*, 2019). If the chalcogen atoms of these functional groups act as halogen bond acceptors, the location of the higher electrostatic potential drives the halogen bond away from the terminus of the thione or selone double bond. Conversely, a chalcogen bond, an interaction analogous to a halogen bond involving the σ hole of a chalcogen atom, can occur at the terminus of the thione or selone double bond (Aakeroy *et al.*, 2019).

As halogen-bond acceptor atoms, nitrogen and oxygen have received considerably more attention than the heavier chalcogens. For example, a survey of the Cambridge Structural Database (CSD, Version 5.42, update 3; Groom *et al.*, 2016), limited to organics, yields 918 results involving an N···I halogen-bond (where the N···I distance less than the sum of the van der Waals radii of the two atoms) to a pyridine-based nitrogen atom. A similar search with urea-, thiourea-, or selenourea-based acceptors yields 36, 100, and 19 results, respectively. Amongst the limited published data involving Se···I interactions, the oxidative addition of interhalogens to diselones, resulting in I–Se–X hypervalent systems is notable (Juárez-Pérez *et al.*, 2011). Our group has been particularly interested in the cooperation of halogen and chalcogen bonding as a versatile crystal engineering tool (Peloquin, McMillen *et al.*, 2021*b*; Peloquin *et al.*, 2021; Peloquin, McMillen *et al.*, 2021*a*)

Motivated by the lack of published structural data involving halogen bonds to thioureas, but especially selenoureas, this work serves to further catalogue the intermolecular interactions of these functionalities with common organoiodines compounds (Scheme 1), as well as to investigate their reactivity and resulting halogen bonding with molecular diiodine. To this end, the sterically encumbered diazepine chalcogenone derivatives hexahydro-1,3-bis(2,4,6-trimethylphenyl)-2H-1,3-diazepine-2-thione (SDiazMesS) and hexahydro-1,3-bis(2,4,6-trimethylphenyl)-2H-1,3-diazepine-2-selone (SDiazMesSe) were prepared, the latter of which has not yet been reported in the synthetic literature, and structurally characterized. These were subsequently utilized as halogen bond acceptors,

to explore their halogen bonding tendencies. Each of these parent molecules was reacted with molecular diiodine, which depending on reaction stoichiometry and solvent choice, provided a variety of C=S-I-I, C=Se-I-I, and C=Se-I derivatives. When acetone was utilized as the reaction solvent with I₂, new S-C, Se-C, and C-C bonds were formed via oxidation by I₂. Utilizing the six most common commercially available halogen bond donors, 1,2-diiodotetrafluorobenzene (1,2-F₄DIB), 1,3-diiodotetrafluorobenzene (1,3-F₄DIB), 1,4-diiodotetrafluorobenzene (1,4-F₄DIB), 1,3,5-triifluorotriiodobenzene (1,3,5-F₃I₃B), iodopentafluorobenzene (IF₅B), and tetraiodoethylene (TIE), the molecular structures of 14 new cocrystals were determined. In most cases, the analogous SDiazMesS and SDiazMesSe cocrystals are isomorphic. No significant Ch···Ch or Ch···I chalogen bonding or I···F halogen bonding is obversed within this series of structures.



Scheme 1 Organic halogen bond acceptors and donors utilized in this study

2. Experimental

2.1. Materials and instrumentation

All reactions were performed under aerobic conditions unless otherwise stated. Solvents were purified and degassed by standard procedures, and all commercially available reagents were used as received. The bis(mesityl) formamidine MesN=CHNHMes (MesForm) was synthesized as reported (Kuhn *et al.*, 2008) and its corresponding diazepinium bromide derivative [SDiazMesH]Br (Kolychev *et al.*, 2009) was prepared by a modification of a literature procedure (Iglesias *et al.*, 2008). ¹H and ¹³C

NMR spectra were obtained on JEOL ECX-300 (300 MHz) or JEOL ECA-500 (500 MHz) FT spectrometers. Chemical shifts are reported in ppm relative to SiMe₄ (δ = 0 ppm) and were referenced internally with respect to the solvent resonances (1 H: δ 2.05 for d₅-acetone; 13 C: δ 29.84 for (CD₃)₂CO; coupling constants are given in hertz (Hz). IR spectra were recorded on a PerkinElmer Spectrum 100 spectrometer using an Attenuated Total Reflectance (ATR) accessory and are reported in cm⁻¹; relative intensities of the absorptions are indicated in parentheses (vs = very strong, s = strong, m = medium, w = weak). Elemental analyses were determined by Atlantic Microlab, Inc. (Norcross, GA).

For single-crystal X-ray analysis, crystals were mounted on low background cryogenic loops using paratone oil. Data were collected using Mo K α radiation ($\lambda = 0.71073$ Å) on a Bruker D8 Venture diffractometer with an Incoatec Ius microfocus source and a Photon 2 detector. Diffraction data were collected using φ and ω -scans and subsequently processed and scaled using the APEX3 (SAINT/SADABS) (Bruker, 2017). The structures were solved with the SHELXT structure solution program and refined utilizing SHELXL, both incorporated in the OLEX2 (v1.5) program package (Sheldrick, 2015b; Dolomanov et al., 2009; Sheldrick, 2015a). Hydrogen atoms were placed in geometrically optimized positions using the appropriate riding models. In (SDiazMesS)•(MeCN), (SDiazMesSe)•(MeCN), (SDiazMesS)•(1,3-F₄DIB), (SDiazMesSe)•(1,3-F₄DIB), 2(SDiazMesS)•(1,3-F₄DIB), $(SDiazMesS) \cdot (1,3,5-F_3I_3B),$ 2(SDiazMesS)•(TIE), 2(SDiazMesSe)•(TIE), positional disorder of the C-C-C portion of the diazepine ring and/or a mesityl substituent was modelled in two parts, utilizing the SIMU restraint as appropriate.

2.2. Preparation of SDiazMesS and SDiazMesSe

The bis(mesityl)formamidine MesN=CHNHMes (MesForm) was synthesized as reported (Kuhn & Grubbs, 2008) and its corresponding diazepinium bromide derivative [SDiazMesH]Br, SDiazMesS, and SDiazMesSe were prepared by a modification of literature procedures (Iglesias *et al.*, 2008; Rais *et al.*, 2016).

2.2.1. **[SDiazMesH]Br.** A stirred mixture of 1,4-dibromobutane (5.939 g, 27.506 mmol), the formamidine MesForm (7.000 g, 24.963 mmol), and potassium carbonate (1.989 g, 14.392 mmol) in acetonitrile (100 mL) was heated to reflux under argon for 24 h. The resulting solution was cooled to room temperature and concentrated under reduced pressure to *ca*. 2 mL to give a very viscous tan residue. Dichloromethane (25 mL) was added to the residue and the mixture stirred overnight, facilitating the separation of a fluffy, white precipitate. The resulting suspension was concentrated under reduced pressure to half volume, treated with cold diethyl ether (60 mL), and the sticky, peach-colored product was isolated by vacuum filtration and dried in vacuo for 24 h (7.820 g, 72%). ¹H NMR data (in CDCl₃): δ 2.27 (s, 6 H, CH₃), 2.41 (s, 12 H, CH₃), 2.56 (m, 4 H, CH₂), 4.65 (m, 4 H,

CH₂), 6.94 (s, 4 H, C₆H₂), 7.21 (s, 1 H, NCHN); 1 H NMR data (in d₆-acetone): δ 2.28 (s, 6 H, CH₃), 2.45 (s, 12 H, CH₃), 2.55 (m, 4 H, CH₂), 4.52 (m, 4 H, CH₂), 7.05 (m, 4 H, C₆H₂), 8.13 (s, 1 H, NCHN).

2.2.2. **SDiazMesS.** A stirred mixture of [SDiazMesH]Br (5.106 g, 12.292 mmol), elemental sulfur (0.433 g, 13.506 mmol), and potassium carbonate (2.208 g, 15.976 mmol) in n-propanol (75 mL) was heated to reflux for 48 h. The resulting yellow suspension was concentrated to ca. 2 mL under reduced pressure to give a beige viscous residue. The product was extracted into dichloromethane (50 mL) and the extract was treated with activated carbon (~1 g) and filtered. The pale orange filtrate was washed with DI water (3 x 30 mL), and the organic phase was dried over magnesium sulfate (~1 g) and filtered. Concentration of the solution under vacuum to ca. 1 mL and addition of hexanes (20 mL) led to the precipitation of the pale brown product, which was separated by filtration and dried in vacuo for 24 h (3.543 g, 79%). Mp = 179-181 °C (dec.). NMR data (in d_6 -acetone): ${}^{1}H \delta 2.09$ (m, 4 H, CH₂), 2.23 (s, 6 H, CH₃), 2.29 (s, 12 H, CH₃), 3.90 (m, 4 H, CH₂), 6.85 (s, 6 H, C₆H₂); 13 C δ 19.0 $(q, {}^{1}J_{C-H} = 126, 4 \text{ C}, CH_3), 20.9 (q, {}^{1}J_{C-H} = 128, 2 \text{ C}, CH_3), 26.4 (t, {}^{1}J_{C-H} = 127, 2 \text{ C}, CH_2), 55.0 (t, {}^{1}J_{C-H} = 128, 2 \text{ C}, CH_3), 26.4 (t, {}^{1}J_{C-H} = 127, 2 \text{ C}, CH_2), 55.0 (t, {}^{1}J_{C-H} = 128, 2 \text{ C}, CH_3), 26.4 (t, {}^{1}J_{C-H} = 127, 2 \text{ C}, CH_2), 55.0 (t, {}^{1}J_{C-H} = 128, 2 \text{ C}, CH_3), 26.4 (t, {}^{1}J_{C-H} = 127, 2 \text{ C}, CH_2), 55.0 (t, {}^{1}J_{C-H} = 128, 2 \text{ C}, CH_3), 26.4 (t, {}^{1}J_{C-H} = 127, 2 \text{ C}, CH_2), 55.0 (t, {}^{1}J_{C-H} = 128, 2 \text{ C}, CH_3), 26.4 (t, {}^{1}J_{C-H} = 127, 2 \text{ C}, CH_2), 55.0 (t, {}^{1}J_{C-H} = 128, 2 \text{ C}, CH_3), 26.4 (t, {}^{1}J_{C-H} = 127, 2 \text{ C}, CH_2), 55.0 (t, {}^{1}J_{C-H} = 128, 2 \text{ C}, CH_3), 26.4 (t, {}^{1}J_{C-H} =$ = 138, 2 C, NCH₂), 130.1 (d, ${}^{1}J_{C-H}$ = 164, 4 C, C_m in C_6H_2), 135.5 (s, 4 C, C_o in C_6H_2), 136.5 (s, 2 C, C_p in C_6H_2), 145.5 (s, 2 C, C_{ipso} in C_6H_2), C=S not observed. IR data: 3141 (w), 2939 (w), 2916 (m), 2854 (w), 2726 (w), 1679 (w), 1643 (s), 1607 (w), 1551 (w), 1488 (m), 1478 (m), 1465 (s), 1426 (m), 1381 (w), 1369 (m), 1359 (w), 1330 (w), 1308 (s), 1287 (vs), 1267 (m), 1214 (m), 1200 (w), 1182 (w), 1148 (w), 1121 (w), 1102 (w), 1032 (w), 1011 (w), 997 (w), 979 (w), 957 (w), 914 (w), 863 (w), 849 (s), 767 (m), 748 (w), 740 (w), 729 (w), 709 (w). Anal. Calc. for C₂₃H₃₀N₂S: C, 75.4; H, 8.3; N, 7.6. Found: C, 76.4; H, 8.2; N, 8.1%. Samples for single-crystal X-ray characterization were obtained from EtOH/DCM or MeCN.

2.2.3. **SDiazMesSe**. A stirred mixture of [SDiazMesH]Br (7.386 g, 17.779 mmol), gray selenium (1.862 g, 23.582 mmol), and potassium carbonate (3.2190 g, 23.291 mmol) in *n*-propanol (150 mL) was heated to reflux for 20 h. The resulting dark red-orange suspension was concentrated to ca. 2 mL under reduced pressure to give a dark orange solid residue. The product was extracted into dichloromethane (30 mL) and the bright yellow-orange extract was washed with DI water (3 x 30 mL). The organic phase was separated, dried over magnesium sulfate (~1 g), filtered, concentrated under vacuum to *ca*. 1 mL, and treated with cold hexanes (10 mL), leading to the precipitation of flaky, orange-yellow product, which was isolated by vacuum filtration and dried in vacuo for 14 h (4.457 g, 61%). Mp = 188-190 °C (dec.). NMR data (in d₆-acetone): 1 H δ 2.15 (m, 4 H, CH₂), 2.23 (s, 6 H, CH₃), 2.30 (s, 12 H, CH₃), 3.93 (m, 4 H, CH₂), 6.86 (s, 6 H, C₆H₂); 13 C δ 19.1 (q, 1 J_{C-H} = 127, 4 C, CH₃), 21.0 (q, 1 J_{C-H} = 127, 2 C, CH₃), 25.7 (t, 1 J_{C-H} = 128, 2 C, CH₂), 55.2 (t, 1 J_{C-H} = 139, 2 C, NCH₂), 130.2 (d, 1 J_{C-H} = 164, 4 C, 2 C in C₆H₂), 135.3 (s, 4 C, 2 C in C₆H₂), 136.7 (s, 2 C, 2 C in C₆H₂), 146.6 (s, 2 C, 2 C_{ipso} in C₆H₂), 186.7 (s, 1 C, C=Se). IR data: 2971 (w), 2945 (w), 2916 (w), 2854 (w),

1737 (m), 1676 (w), 1645 (s), 1607 (w), 1550 (w), 1489 (m), 1471 (s), 1430 (m), 1369 (m), 1360 (m), 1331 (m), 1286 (vs), 1275 (w), 1254 (w), 1215 (s), 1203 (w), 1185 (w), 1149 (w), 1121 (w), 1104 (w), 1032 (w), 1012 (w), 998 (w), 981 (w), 902 (w), 864 (w), 850 (s), 775 (w), 755 (w), 743 (w), 707 (w). Anal. Calc. for C₂₃H₃₀N₂Se: C, 66.8; H, 7.3; N, 6.8. Found: C, 66.7; H, 7.4; N, 6.7%. Samples for single-crystal X-ray characterization were obtained from EtOH/DCM or MeCN.

2.3. Reaction of SDiazMesS and SDiazMesSe with l2

2.3.1. **(SDiazMesS)l₂**. Diethyl ether (10 mL) was added to a mixture of SDiazMesS (0.150 g, 0.409 mmol) and elemental iodine (0.104 g, 0.405 mmol), resulting in the formation, within minutes, of a dark orange solid and a dark red solution. After stirring the suspension for 17 h, the product was isolated by filtration and dried in vacuo for 24 h (0.154 g, 61%). Mp = 141-143 °C (dec.). NMR data (in d₆-acetone): 1 H δ 2.27 (s, 10 H, CH₃ + CH₂), 2.37 (s, 12 H, CH₃), 4.12 (s, 4 H, CH₂) 6.96 (s, 4 H, C₆H₂); 13 C δ 18.5 (q, 1 J_{C-H} = 127, 4 C, CH₃), 20.5 (q, 1 J_{C-H} = 128 , 2 C, CH₃), 23.7 (t, 1 J_{C-H} = 130, 2 C, CH₂), 54.7 (t, 1 J_{C-H} = 143, 2 C, CH₂), 129.6 (d, 1 J_{C-H} = 157, 4 C, 2 C m in C₆H₂), 133.7 (d, 2 J_{C-H} = 6, 4 C, 2 C in C₆H₂), 136.7 (s, 2 C, 2 C m in C₆H₂), 142.6 (s, 2 C, 2 C m in C₆H₂), 176.3 (s, 1 C, C=S). IR data: 2948 (w), 2910 (w), 2868 (w), 2730 (w), 1608 (w), 1506 (s), 1474 (m), 1452 (w), 1432 (m), 1391 (m), 1373 (w), 1365 (w), 1354 (w), 1337 (m), 1306 (s), 1286 (vs), 1270 (vs), 1211 (w), 1202 (w), 1187 (w), 1153 (w), 1105 (w), 1036 (w), 1014 (w), 999 (w), 978 (w), 966 (w), 937 (w), 926 (w), 910 (w), 892 (w), 853 (s), 841 (m), 798 (w), 756 (m), 745 (w), 729 (w), 706 (w). Anal. Calc for C₂₃H₃₀I₂N₂S: C, 44.5; H, 4.9; N, 4.5. Found: C, 44.3; H, 4.9; N, 4.5%. Crystals suitable for X-ray diffraction analysis were obtained through the slow evaporation of an ethanolic solution of the compound.

2.3.2. (**SDiazMesSe)**₁₂. A mixture of SDiazMesSe (0.144 g 0.349 mmol) and elemental iodine (0.093 g, 0.366 mmol) in diethyl ether (10 mL) was stirred overnight at room temperature. The resulting reddish-brown suspension was concentrated under reduced pressure to ca. 1 mL, treated with diethyl ether (5 mL), and the dark orange product was isolated by filtration, washed with diethyl ether (2 mL), and dried in vacuo for 18 h (0.210 g, 91%). Mp = 195-198 °C (dec.). ¹H NMR data (in d₆-acetone): δ 2.28 (s, 3 H, CH₃), 2.33 (s, 4 H, CH₂), 2.37 (s, 6 H, CH₃), 4.22 (s, 4 H, CH₂), 6.98 (s, 2 H, C₆H₂); 13 C NMR data (in d₆-DMSO): δ 17.9 (q, $^{1}J_{C-H}$ = 128, 4 C, CH₃), 20.0 (q, $^{1}J_{C-H}$ = 127, 2 C, CH₂), 22.6 (t, $^{1}J_{C-H}$ = 131, 2 C, CH₂), 55.5 (t, $^{1}J_{C-H}$ = 146, 2 C, CH₂), 129.5 (d, $^{1}J_{C-H}$ = 158, 2 C, $^{2}C_{C}$ in C₆H₂), 133.4 (s, $^{1}J_{C-H}$ = 160, 4 C, $^{2}C_{C}$ in C₆H₂), 138.1 (s, 4 C, $^{2}C_{C}$ in C₆H₂), 142.2 (s, 2 C, $^{2}C_{C}$ in C₆H₃), C=Se not observed. IR data: 2950 (m), 2911 (m), 2854 (w), 2730 (w), 1777 (w), 1739 (w), 1607 (m), 1516 (s), 1474 (s), 1452 (w), 1434 (s), 1392 (m), 1374 (m), 1365 (m), 1355 (w), 1338 (m), 1308 (w), 1293 (vs), 1282 (vs), 1269 (vs), 1261 (vs), 1210 (m), 1189 (m), 1150 (w), 1104 (m), 1035 (m), 998 (m), 979 (w), 957 (w), 938 (w), 923 (w), 896 (w), 853 (s), 739 (m), 704 (w). Anal. Calc. for C₂₃H₃₀I₂N₂Se: C, 41.4; H, 4.5; N, 4.2. Found: C, 41.1; H, 4.7; N, 4.1%. Crystals suitable for X-ray

diffraction analysis were obtained through the slow evaporation of an ethanolic solution of the compound.

2.4. Preparation of cocrystals

- **2.4.1.** (SDiazMesS)•(1,2-F₄DIB). In a 20 mL glass vial, SDiazMesS (30 mg, 0.082 mmol) and 1,2-F₄DIB (33 mg, 0.082 mmol) were dissolved in a 1:1 mixture of ethanol and dichloromethane (5 mL) with gentle heating. The solvent was allowed to slowly evaporate under ambient conditions (18–20 °C) until colorless, needle-like crystals were observed.
- **2.4.2.** (SDiazMesS)•(1,3-F₄DIB). Using the same procedure as (SDiazMesS)•(1,2-F₄DIB), SDiazMesS (30 mg, 0.082 mmol) and 1,3-F₄DIB (66 mg, 0.16 mmol) were combined to yield colorless, plate-like crystals.
- 2.4.3. (SDiazMesSe)•(1,3-F₄DIB). Using the same procedure as (SDiazMesS)•(1,2-F₄DIB), SDiazMesSe (30 mg, 0.073 mmol) and 1,3-F₄DIB (58 mg, 0.15 mmol) were combined to yield yellow, needle-like crystals.
- 2.4.4. **2(SDiazMesS)•(1,3-F₄DIB)**. Using the same procedure as **(SDiazMesS)•(1,2-F₄DIB)**, SDiazMesS (60 mg, 0.16 mmol) and 1,3-F₄DIB (33 mg, 0.082 mmol) were combined to yield colorless, needle-like crystals.
- 2.4.5. **2(SDiazMesSe)•(1,3-F4DIB)**. Using the same procedure as **(SDiazMesS)•(1,2-F4DIB)**, SDiazMesS (60 mg, 0.15 mmol) and 1,3-F4DIB (29 mg, 0.073 mmol) were combined to yield colorless, needle-like crystals.
- 2.4.6. **2(SDiazMesS)•(1,4-F₄DIB)**^t and **2(SDiazMesS)•(1,4-F₄DIB)**^m. Using the same procedure as **(SDiazMesS)•(1,2-F₄DIB)**, SDiazMesS (60 mg, 0.16 mmol) and 1,4-F₄DIB (33 mg, 0.082 mmol) were combined to yield **2(SDiazMesS)•(1,4-F₄DIB)**^t as colorless, needle-like crystals on the sides of the vial and **2(SDiazMesS)•(1,4-F₄DIB)**^m as colorless, plank-like crystals from the bottom surface of the vial.
- 2.4.7. **2(SDiazMesSe)•(1,4-F₄DIB)**^t. Using the same procedure as **(SDiazMesS)•(1,2-F₄DIB)**, SDiazMesSe (60 mg, 0.15 mmol) and 1,4-F₄DIB (29 mg, 0.073 mmol) were combined to yield colorless, plank-like crystals.
- 2.4.8. (SDiazMesS)•(1,3,5-F₃I₃B). Using the same procedure as (SDiazMesS)•(1,2-F₄DIB), SDiazMesS (30 mg, 0.082 mmol) and 1,3,5-F₃I₃B (42 mg, 0.082 mmol) were combined to yield colorless, needle-like crystals.

- 2.4.9. (SDiazMesSe)•(1,3,5-F₃I₃B). Using the same procedure as (SDiazMesS)•(1,2-F₄DIB), SDiazMesSe (30 mg, 0.073 mmol) and 1,3,5-F₃I₃B (37 mg, 0.073 mmol) were combined to yield yellow, needle-like crystals.
- 2.4.10. (SDiazMesS)•(IF₅B). Using the same procedure as (SDiazMesS)•(1,2-F₄DIB), SDiazMesS (30 mg, 0.082 mmol) and IF₅B (120 mg, 0.41 mmol) were combined to yield colorless, plate-like crystals.
- **2.4.11. 2(SDiazMesSe)•5(IF₅B).** In a 1 mL glass tube, SDiazMesSe (30 mg, 0.073 mmol) was dissolved in IF₅B (0.25 mL, 1.8 mmol). The solution was allowed to slowly evaporate under ambient conditions, yielding yellow, plate-like crystals after approximately 1 week.
- 2.4.12. **2(SDiazMesS)•(TIE).** Using the same procedure as **(SDiazMesS)•(1,2-F₄DIB)**, SDiazMesS (60 mg, 0.16 mmol) and TIE (44 mg, 0.082 mmol) were combined to yield yellow, plate-like crystals.
- 2.4.13. **2(SDiazMesSe)•(TIE).** Using the same procedure as **(SDiazMesS)•(1,2-F₄DIB)**, SDiazMesSe (60 mg, 0.15 mmol) and TIE (39 mg, 0.073 mmol) were combined to yield yellow, block-like crystals.

3. Results and Discussion

3.1. Synthesis of SDiazMesS and SDiazMesSe

The N-heterocyclic chalcogenones SDiazMesE (E = S, Se), envisioned to have good solubility in common organic solvents and exhibit simple ¹H and ¹³C NMR spectra to facilitate characterization of products, were synthesized in three steps (Scheme 2). Commercially available 2,4,6-trimethylaniline (mesitylamine) was reacted neat with triethylorthformate in the presence of a catalytic amount of acetic acid (Kuhn & Grubbs, 2008) to produce the bis(mesityl) formamidine MesN=CHNHMes (MesForm) in ~80% yield. The formamidine was then reacted with 1,4-dibromobutane and potassium carbonate in refluxing acetonitrile (Iglesias *et al.*, 2008) to generate the diazepinium bromide derivative [SDiazMesH]Br, which was isolated in ~70% yield. Finally, the diazepinium salt is reacted with either elemental sulfur or gray selenium in the presence of a base (K₂CO₃) in refluxing n-propanol to form the desired thione and selone products in 60-80% yield. The two chalcogenones were fully characterized by a combination of analytical and spectroscopic techniques, including elemental analysis, IR and ¹H & ¹³C NMR spectroscopies, and single-crystal X-ray diffraction, as described in the next section.

Scheme 2 Synthesis of N-heterocyclic chalcogenones SDiazMesE (E = S, Se)

3.2. Structure of SDiazMesS and SDiazMesSe and their MeCN solvates

The parent compound **SDiazMesS** crystallizes in the monoclinic space group $P2_1/c$, whereas SDiazMesSe crystallizes in the orthorhombic space group Pbca. The thiourea and selenourea are prominent in the respective structures, with a C=S length of 1.6887(13) Å and an average C=Se length of 1.850(4) Å from the two unique molecules in the asymmetric unit. (Table 1) Despite the cyclic nature of the molecules' core, the N-C=E (E = S, Se) angle remains at approximately 120°, consistent with that of an isolated thiourea or selenourea molecule (Tomkowiak & Katrusiak, 2018). In **SDiazMesS**, weak C-H···S hydrogen bonds (C···S = 3.7030(15) Å and 3.4858(14) Å), involving hydrogen atoms of the heterocyclic ring, contribute to the stacking of molecules along the c axis. With two unique molecules in the asymmetric unit of SDiazMesSe, the hydrogen-bonding pattern is more complex. To one selenium atom, weak C–H···Se hydrogen bonds (C···Se = 3.671(2) Å and 3.665(2)Å) are observed to two different molecules, both involving hydrogen atoms of the heterocyclic rings. In both cases, the mesityl rings are nearly perpendicular to the urea plane. For example, in SDiazMesS, the mesityl-to-urea plane angles are 91.46(4)° and 89.60(4)°. These geometric parameters remain consistent throughout the variety of cocrystals, adducts, and solvates in this study. Unlike the unsolvated structures of the parent molecules, the acetonitrile solvates (SDiazMesS)•(MeCN) and (SDiazMesSe)•(MeCN) are isomorphous, with a weak hydrogen bonding interaction observed between the chalcogen atom and the acetonitrile molecule.

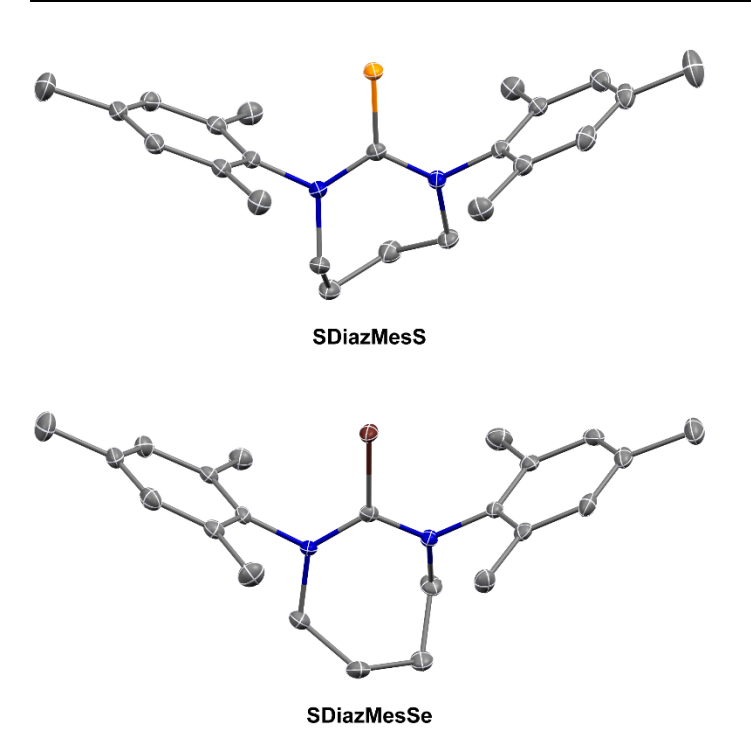


Figure 1 Molecular structure of **SDiazMesS** and **SDiazMesSe**. Displacement ellipsoids are drawn at the 50% probability level. Hydrogen atoms are omitted for clarity.

$_{\rm 3.3.}$ Reaction of SDiazMesS and SDiazMesSe with $I_{\rm 2}$

$$E = S, Se$$

$$I_{2}$$

$$E = S, Se$$

$$I_{2}$$

$$E = S, Se$$

$$I_{3}$$

$$I_{2}$$

$$I_{2}$$

$$I_{2}$$

$$I_{3}$$

$$I_{3}$$

$$I_{3}$$

$$I_{3}$$

$$I_{4}$$

$$I_{5}$$

$$I_{5}$$

$$I_{5}$$

$$I_{6}$$

$$I_{7}$$

$$I_{13}$$

Scheme 3 Reactions of SDiazMesE (E = S, Se) with I_2

The reaction of molecular iodine with **SDiazMesS** and **SDiazMesSe** provided a rich series of products depending on the ratio of I_2 to thione or selone and the solvent choice (Scheme 3). The reaction of **SDiazMesS** or **SDiazMesSe** with a stoichiometric amount of I_2 in diethyl ether provides **SDiazMesS-I₂** or **SDiazMesSe-I₂**, both crystallizing in the triclinic space group P-1. In both cases, short chalcogen···iodine distances are observed (S–I = 2.6738(9) Å and Se–I = 2.7559(4) Å), with concomitant lengthening of the I–I bond at 2.8794(4) Å in **SDiazMesS-I₂** and 2.9106(4) Å in **SDiazMesSe-I₂**. These I–I distances correspond to bond orders of 0.59 and 0.53 respectively, as calculated using the expression of Pauling, $D(n') = D(1) - 0.71 \log (n')$ with a D(1) of 2.72 Å (Pauling, 1960). A series of weak C–H···I hydrogen bonds consolidate the packing.

The reaction with 2.5 molar equivalents of I_2 in a 1:1 mixture of ethanol and dichloromethane provides different products from **SDiazMesS** and **SDiazMesSe**. When the reaction was conducted with **SDiazMesS**, the cocrystal (**SDiazMesS–I_2**)•(I_2) was obtained in the triclinic space group P-1. The bond distances within the S–I–I fragment are reduced from those in **SDiazMesS**, with the S–I

distance shrinking to 2.5052(5) Å while the I-I distance further elongates to 3.0803(4) Å. This change in bond geometries is indicative of further progression towards the dipolar I+···I- extreme, with a calculated bond order of 0.31. The consolidation of the negative charge on the terminal iodine atom of the S-I-I fragment contributes to its increased ability to serve as a halogen bond acceptor. The incorporation of a diiodine molecule within the structure aids in the formation of chains in the [0 -1 1] direction through I···I halogen bonding. There are two such unique I···I halogen bonds formed at each terminal iodine atom of the S-I-I, both of which are similar in length ($I \cdot \cdot \cdot I = 3.4171(4)$ Å and 3.4694(5) Å). In contrast to the reaction of **SDiazMesS** with excess I₂, the reaction of 2.5 molar equivalents of I₂ with **SDiazMesSe** in 1:1 ethanol:dicholormethane provides the salt **[(SDiazMesSe**- $I(I_3)$]. Crystalline [(SDiazMesSe-I)(I_3)] forms within five minutes, and if this material is recrystallized from dichloromethane, the crystalline solvate [(SDiazMesSe-I)(I₃)]•(DCM) is obtained. In both cases, the Se-I-I fragment is better represented as (Se-I⁺)(I₃⁻). This assignment is supported by the further contraction of the Se-I distance to 2.5807(14) Å and expansion of the I⁺···I distance to 3.2052(10) Å relative to SDiazMesSe-I₂. This I···I distance would correspond to a calculated bond order of only 0.20. The C=Se length remains relatively unchanged (1.921(10) Å) compared to SDiazMesSe-I₂ (1.8973(16) Å. The triiodide anion in both salts is asymmetric, with the two I-I lengths of 3.0222(10) Å and 2.8492(10) Å in [(SDiazMesSe-I)(I₃)] and 3.0098(6) Å and 2.8426(6) Å in [(SDiazMesSe-I)(I₃)]•(DCM). This degree of asymmetry is in line with other reported triiodide salts (Kobra et al., 2018). In [(SDiazMesSe-I)(I₃)], halogen bonding does not contribute to the long-range packing motif, beyond the aforementioned connection of one end of I₃⁻ to the Se-I fragment; however, in [(SDiazMesSe-I)(I₃)]•(DCM), a combination of I···I halogen bonding and Se...I chalcogen bonding contributes to the formation of chains along the a axis (Figure 2).

The use of acetone as the reaction solvent allowed access to new organic products resulting from forming a new covalent bond between the chalcogen atom and a methyl carbon of acetone. When the reaction of **SDiazMesSe** and 2.5 molar equivalents of diiodine was conducted in acetone, the salt **[(SDiazMesSe-DMK)(I₃)]•(I₂)** was obtained, displaying an added dimethylketone (DMK) fragment, resulting from the diiodine-promoted addition of an acetone molecule to the selenium atom. The only slight elongation of the C=Se bond and negligible change in the C-N lengths suggest the positive charge is primarily localized to the selenium atom (Table 1). If a 1:1 mixture of ethanol and acetone was utilized as the reaction solvent for the reaction with 2.5 molar equivalents of I₂, the isomorphic products **[(SDiazMesS-MIBK)(I₃)]** and **[(SDiazMesSe-MIBK)(I₃)]** were obtained, both crystallizing in the triclinic space group *P*-1. The methylisobutylketone (MIBK) fragment bound to the chalcogen atom results from the further bond formation of the methyl carbon of **[(SDiazMesSe-DMK)(I₃)]•(I₂)** with the carbonyl carbon of an additional acetone molecule along with deoxygenation. A related reaction involved the addition of acetone to a sulfur atom in 1,4-dithiane has been previous reported (Peloquin *et al.*, 2021). Just as in **[(SDiazMesSe-DMK)(I₃)]•(I₂)**, the only

slight lengthening of C-S and C-Se distances, along with a negligible change in C-N distances, relative to the parent molecule indicate the positive charge is primarily localized to the chalcogen atom. The triiodide anion is pinned in place by weak Type I halogen bonds with the I₂ molecule. While all attempts to isolate the analogous **SDiazMesS**-containing structure to **[(SDiazMesSe-DMK)(I₃)]**•(**I₂)** were unsuccessful, the isolation of **[(SDiazMesS-MIBK)(I₃)]** does suggest its formation occurs. Adding ethanol to the reaction mixture reduces the overall solvent polarity and likely supports the solubility of the increased aliphatic character of the MIBK fragment over DMK.

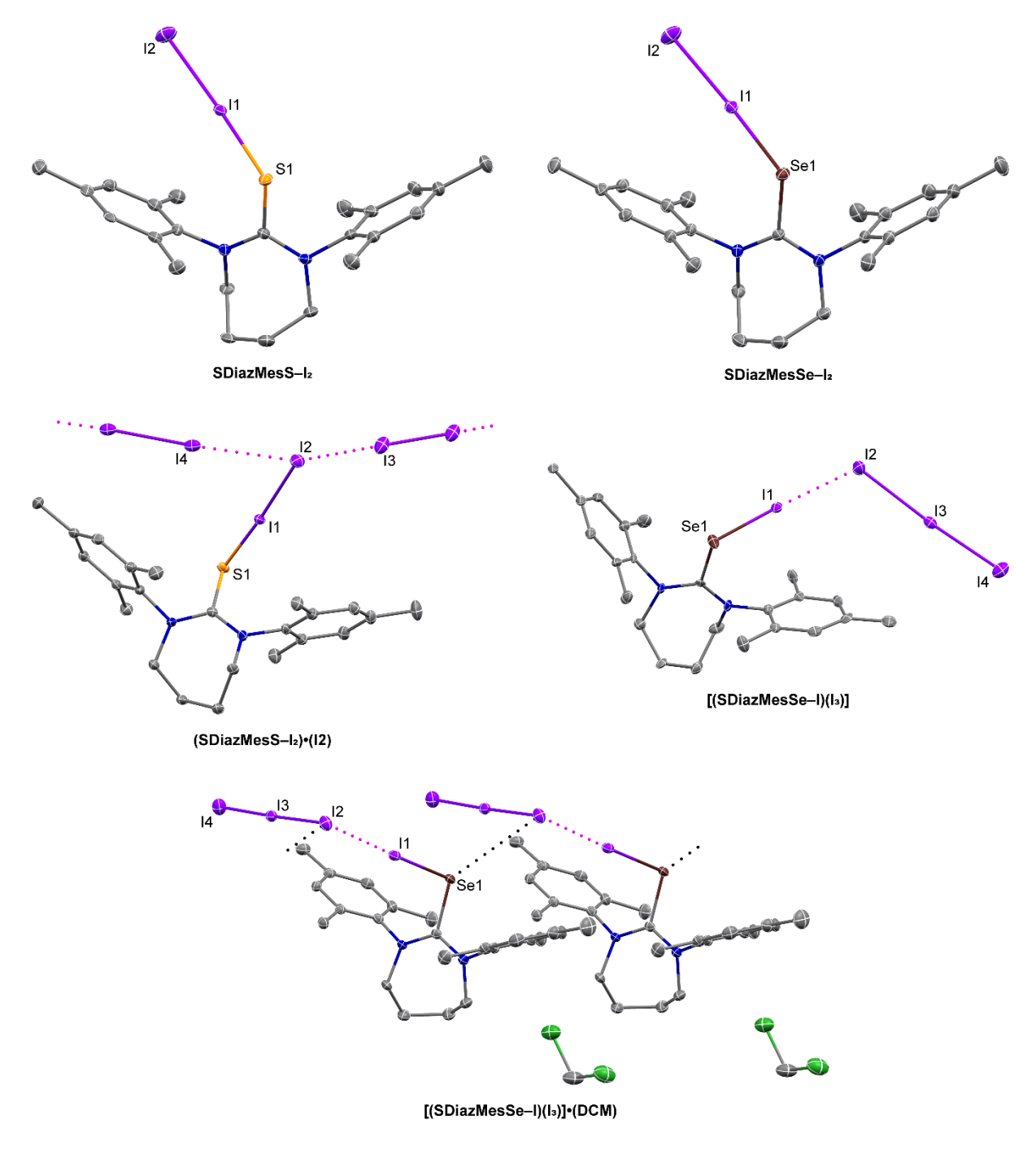


Figure 2 Molecular structure of the products of the reaction of I_2 with SDiazMesS and SDiazMesSe in non-acetone solvents. Intermolecular $I \cdots I$ and $Se \cdots I$ interactions are indicated by magenta and

black dotted lines, respectively. Displacement ellipsoids are drawn at the 50% probability level. Hydrogen atoms are omitted for clarity.

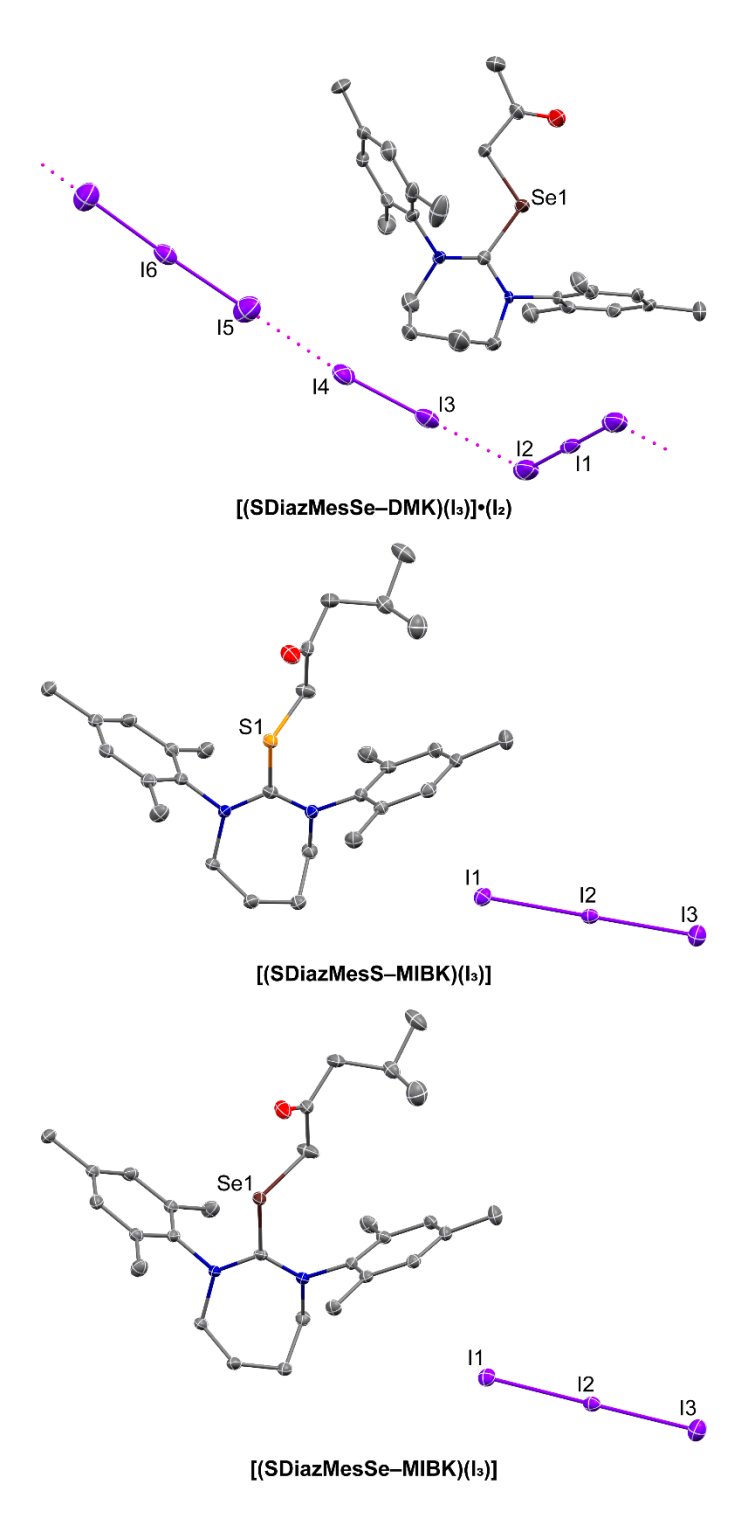


Figure 3 Molecular structure of the products of the reaction of I_2 with SDiazMesS and SDiazMesSe in acetone. Intermolecular $I\cdots I$ interactions are indicated by magenta dotted lines. Displacement ellipsoids are drawn at the 50% probability level. Hydrogen atoms are omitted for clarity.

3.4. Cocrystallization of SDiazMesS and SDiazMesSe with iodofluorobenzenes

The cocrystal (SDiazMesS)•(1,2-F₄DIB) crystallizes in the orthorhombic space group *Pna2*₁ with one molecule each of SDiazMesS and 1,2-F₄DIB within the asymmetric unit (Fig. 1). C–I···S halogen bonding occurs between the thione sulfur atom and only one iodine atom of 1,2-F₄DIB, leading to the formation of discrete halogen bonded dimers. The halogen-bond distance in this cocrystal, 3.2092(12) Å, is significantly shorter than measured in the ternary cocrystal of thiourea, 1,2-F₄DIB, and 18-crown-6 (3.4680(6) Å) (Topić & Rissanen, 2016). The lack of I···S halogen bonding to the second iodine atom is likely due to a combination of the steric bulk of SDiazMesS and the proximity of the iodine atoms in 1,2-F₄DIB. Neighboring dimers consolidate through a combination of weak C–H···I and C–H···S interactions. All attempts to isolate the corresponding SDiazMesSe cocrystal were unsuccessful.

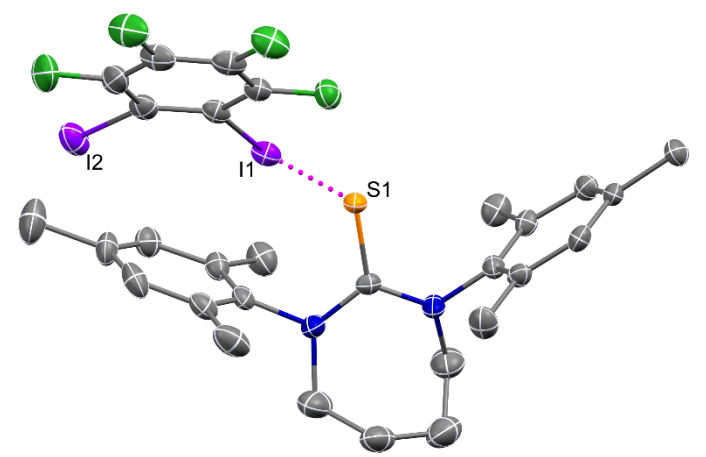


Figure 4 Halogen bonding in **(SDiazMesS)•(1,2-F₄DIB)**. Intermolecular I···S halogen bonding is indicated by magenta dotted lines. Displacement ellipsoids are drawn at the 50% probability level. Hydrogen atoms are omitted for clarity.

With 1,3-F₄DIB as the halogen bond donor, four cocrystalline structures were obtained (Fig. 2). The first two, (SDiazMesS)•(1,3-F₄DIB) and (SDiazMesSe)•(1,3-F₄DIB), are isomorphic. Both cocrsytals are obtained in the orthorhombic space group $P2_12_12_1$ with one molecule of either SDiazMesS or SDiazMesSe along with one molecule of 1,3-F₄DIB. A pair of nearly identical length C–I···S halogen bonds connect SDiazMesS or SDiazMesSe molecules with molecules of 1,3-F₄DIB in alternating fashion to form helical chains propagating along the b axis. The packing is consolidated along the a axis by weak C–H··· π interactions and in the c direction by C–H···F interactions, both involving hydrogen atoms of the heterocyclic ring. The addition of a second equivalent of SDiazMesS or SDiazMesSe results in the cocrystals 2(SDiazMesS)•(1,3-F₄DIB) and 2(SDiazMesSe)•(1,3-F₄DIB). Just as in the 1:1 cocrystals, the 2:1 cocrystals are isomorphic with one another, crystallizing in the monoclinic space group C2/c. Discrete halogen bonding units are formed with only one halogen bond observed at each chalcogen atom. These units stack along the c axis through π ··· π stacking of the 1,3-F₄DIB rings, with ring plane-to-ring plane distances of 3.2840(10) Å and 3.3046(12) Å and slippage of 2.359 Å and 2.337 Å in 2(SDiazMesS)•(1,3-F₄DIB) and 2(SDiazMesSe)•(1,3-F₄DIB)

respectively. These four cocrystals represent the first reported examples of halogen-bonded cocrystals of 1,3-F₄DIB with a thiourea or selenourea.

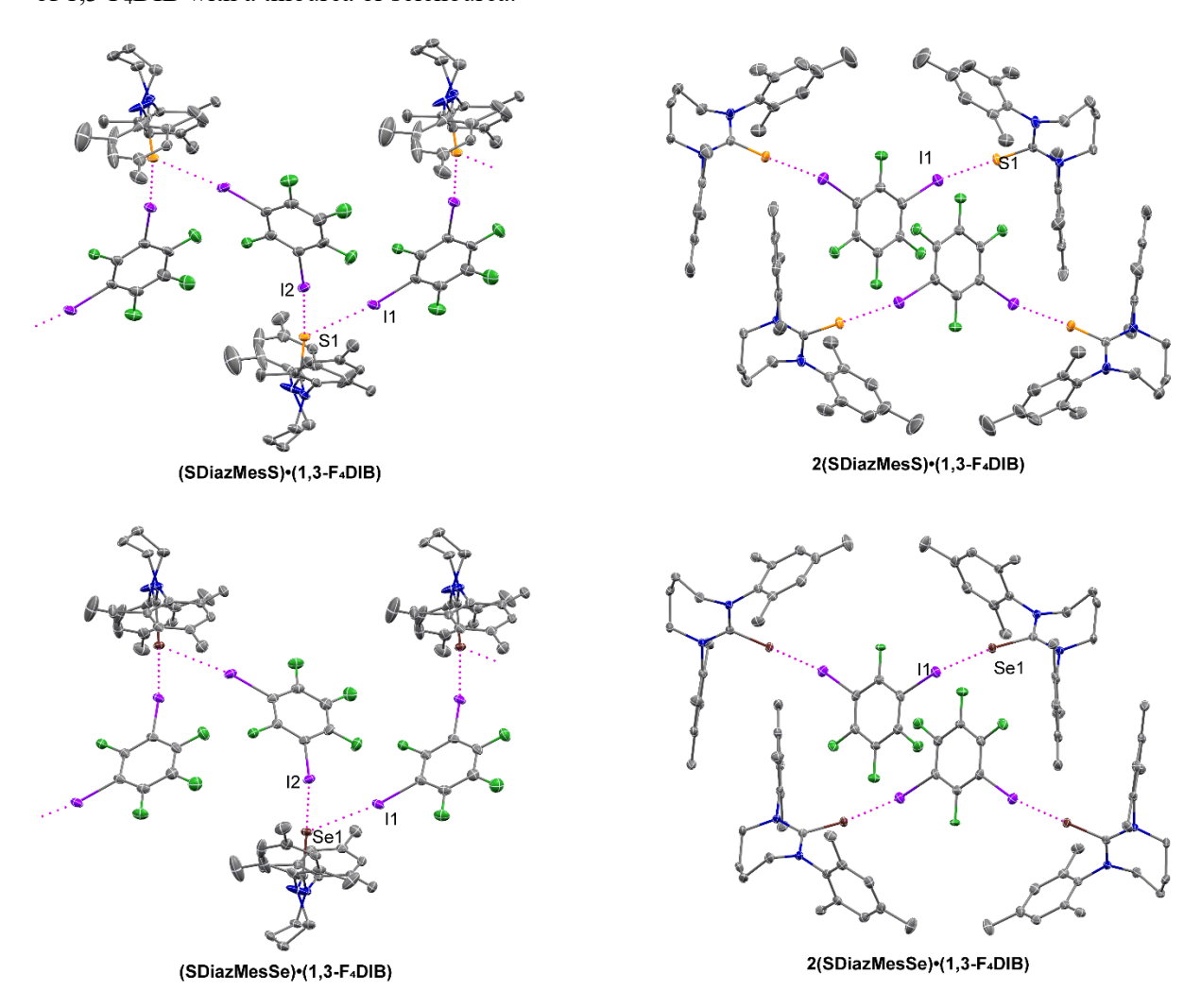
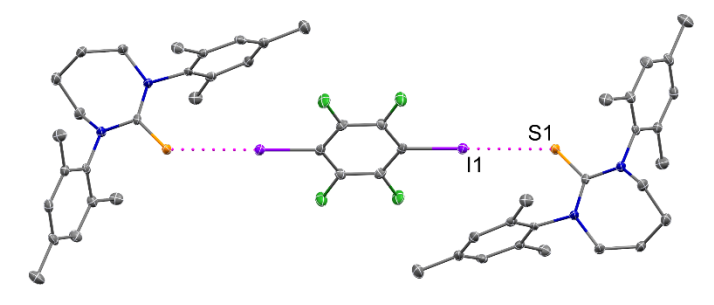


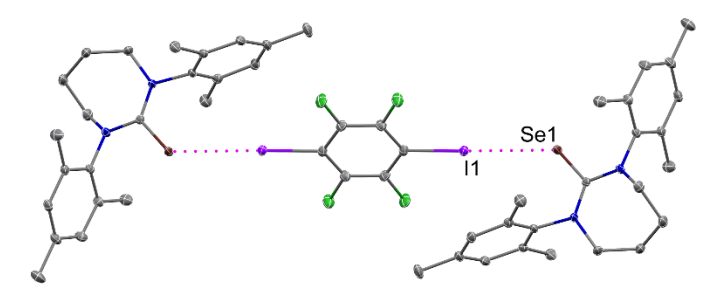
Figure 5 Halogen bonding in the 1,3-F₄DIB containing cocrystals. Intermolecular I···S and I···Se halogen bonding is indicated by magenta dotted lines. Displacement ellipsoids are drawn at the 50% probability level. Hydrogen atoms are omitted for clarity.

The reaction with the common halogen bond donor 1,4-F₄DIB yielded two polymorphic structures with SDiazMesS: **2(SDiazMesS)•(1,4-F₄DIB)**^t, which crystallized in the triclinic space group *P*-1, and **2(SDiazMesS)•(1,4-F₄DIB)**^m which crystallized in the monoclinic space group *P*2₁/*c*. The triclinic isomorph, **2(SDiazMesSe)•(1,4-F₄DIB)**^t, was obtained with SDiazMesSe (Fig. 3). All attempts to isolate the monoclinic isomorph with SDiazMesSe were unsuccessful. In all three cases, a single halogen bond is observed at each chalcogen atom, forming discrete units from 2 thione or selone molecules and one molecule of 1,4-F₄DIB. For the triclinic isomorphs, the halogen bond geometry is nearly linear, with a C–I···S angle of 175.67(9)° in **2(SDiazMesS)•(1,4-F₄DIB)**^t and a C–I···Se angle of 173.97(4)° in **2(SDiazMesSe)•(1,4-F₄DIB)**^t. The iodine···chalcogen distances in these triclinic polymorphs (I···S = 3.2318(7) Å and I···Se = 3.2553(3) Å) are shorter than the

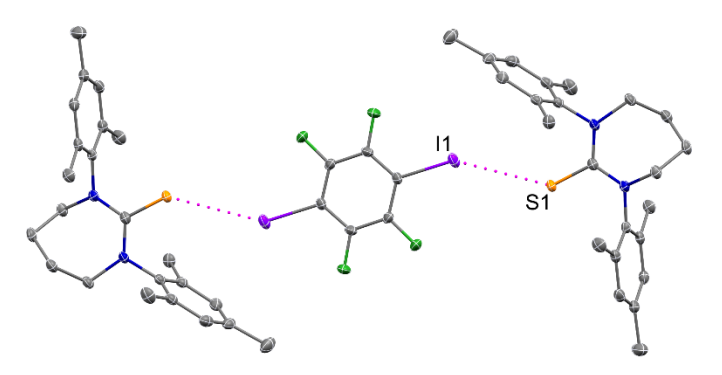
analogous cocrystals with thiourea (I···S = 3.287(12) Å) or selenourea (I···Se = 3.3151(17) Å) (Arman *et al.*, 2010; Chernysheva & Haukka, 2021). Weak chalcogen···hydrogen interactions contribute to the stacking of these discrete units along the *a* axis. In the monoclinic polymorph, while the discrete 2:1 halogen bonding units are maintained, the C–I···S halogen bond is elongated relative to the triclinic polymorph, and deviates significantly from linearity (143.57(6)°). This geometric arrangement may suggest an intermediate between true halogen and chalcogen bonds. The C–I iodine atom is also involved in a weak I··· π interaction (3.646(2) Å). The repositioning of the 1,4-F₄DIB between the two SDiazMesS molecules in the monoclinic polymorph compared to the triclinic polymorph enable the iodine atoms to be involved in weak I··· π interactions (3.646(2) Å).



2(SDiazMesS)•(1,4-F₄DIB)^t



2(SDiazMesSe)•(1,4-F₄DIB)^t

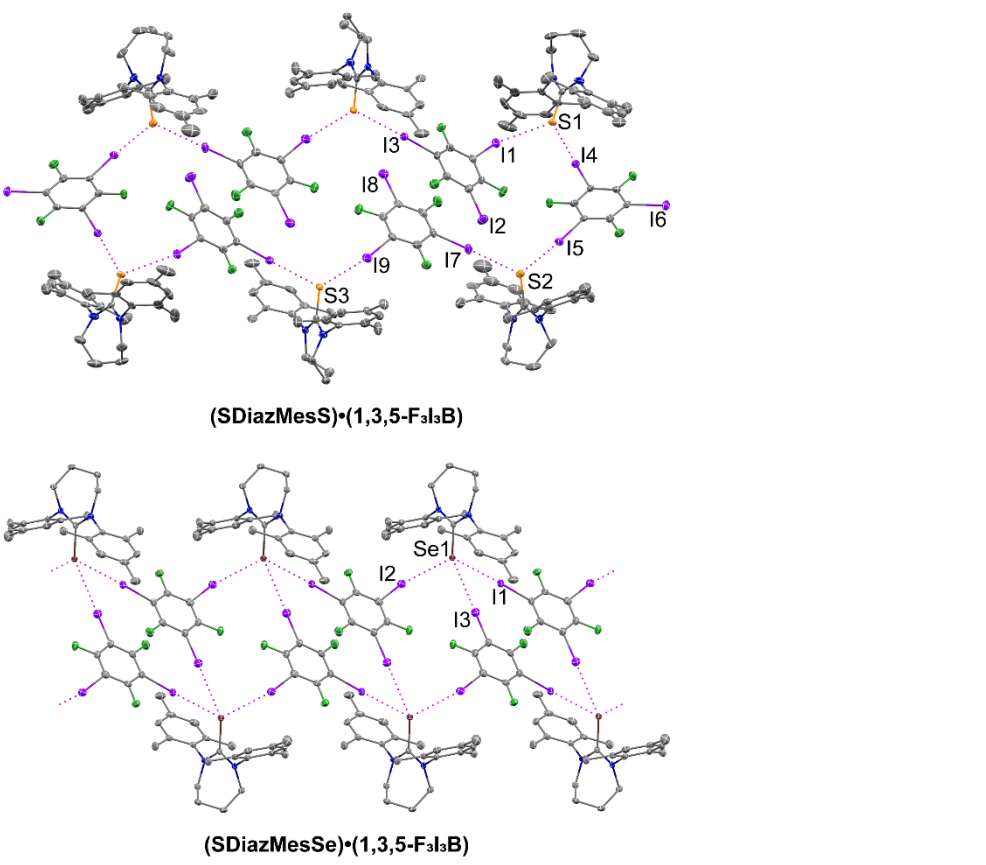


2(SDiazMesS)•(1,4-F₄DIB)^m

Figure 6 Halogen bonding in the 1,4-F₄DIB containing cocrystals. Intermolecular I···S and I···Se halogen bonding is indicated by magenta dotted lines. Displacement ellipsoids are drawn at the 50% probability level. Hydrogen atoms are omitted for clarity.

While the diiodotetrafluorobenzene-containing cocrystal systems discussed thus far show roughly equivalent behaviour between sulfur and selenium, the 1,3,5-F₃I₃B cocrystals $(SDiazMesS) \bullet (1,3,5-F_3I_3B)$ and $(SDiazMesSe) \bullet (1,3,5-F_3I_3B)$ do display a subtle, but important difference (Fig. 4). In this pair, the structures are not isomorphic, with (SDiazMesS)•(1,3,5-F₃I₃B) crystallizing in the monoclinic space group P2₁/c and (SDiazMesSe)•(1,3,5-F₃I₃B) in space group $P2_1/n$. In both cases, a pair of iodine ··· chalcogen halogen bonds are observed at each chalcogen atom. Each of these interactions ranges in normalized distance parameter, R_{XB}, from 0.85 to 0.92. The third iodine atom of each 1,3,5-F₃I₃B molecule drives the differences in the overall packing motif. Of the three symmetry unique 1,3,5-F₃I₃B molecules in (SDiazMesS)•(1,3,5-F₃I₃B), the third iodine atom of two of these (I2 and I8) have the appropriate geometric orientation to participate in a C-I···S halogen bond (C-I···S = 170.5(2)° and 177.9(2)° respectively), but the iodine···sulfur distance is well beyond the sum of the van der Waals radii ($R_{XB} = 1.12$ and 1.14 respectively). This series of interactions contributes to the formation of ring-link units consisting of six SDiazMesS and six 1,3,5-F₃I₃B molecules. The third iodine atom of the final symmetry unique 1,3,5-F₃I₃B molecule participates in a weak type I, I···I interaction. In (SDiazMesSe)•(1,3,5-F₃I₃B), two primary C-I···Se halogen bonds $(R_{\rm XB} = 0.90 \text{ and } 0.92)$ again occur at each selenium atom. However, the third iodine atom of each 1,3,5-F₃I₃B molecule drives a difference in the overall packing motif. In this case, a weak C-I···Se halogen bond occurs roughly at the sum of the van der Waals radii ($R_{XB} = 1.01$). This weak contact, likely enabled by the increased van der Waals radii of selenium over sulfur, and therefore decreased

steric congestion around the chalcogen atom, is enough to consolidate the halogen bonding motif into a ladder-like chain propagating in the c direction. These two cocrystals represent the first reported



examples of halogen-bonded cocrystals of 1,3,5-F₃I₃B with a thiourea or selenourea.

Figure 7 Halogen bonding in the 1,3,5- F_3I_3B containing cocrystals. Intermolecular I···S and I···Se halogen bonding is indicated by magenta dotted lines. Displacement ellipsoids are drawn at the 50% probability level. Hydrogen atoms are omitted for clarity.

With the halogen bond donor iodopentafluorobenzene (IF₅B), different reaction conditions were required for **SDiazMesS** and **SDiazMesSe**, resulting in dramatically different cocrystalline structures. By reacting 5 equivalents of IF₅B with SDiazMesS in ethanol, (**SDiazMesS)•(IF₅B)** was obtained in the orthorhombic space group $Pna2_1$. A single I···S halogen bond is observed at each sulfur atom. The halogen bond length (I···S = 3.1809(14) Å) is comparable to that measured in the ternary cocrystal of IF₅B, thiourea, and 18-crown-6 (I···S = 3.1977(14) Å) (Topić & Rissanen, 2016). These halogen bonded pairs stack along the a axis through π ··· π stacking of the IF₅B molecules, with a centroid to centroid distance between rings of 3.0340(19) Å and slippage of 2.925 Å. The reaction conditions which produced (**SDiazMesS)•(IF₅B)** did not yield the analogous cocrystal with **SDiazMesSe**. To force cocrystallization, **SDiazMesSe** was dissolved in neat IF₅B, resulting in the cocrystal **2(SDiazMesSe)•5(IF₅B)**. This cocrystal was obtained in the monoclinic space group $P2_1/c$. In contrast to (**SDiazMesS)•(IF₅B)**, in which only one halogen bond is observed to each chalcogen atom, two I···Se halogen bonds are observed to each selenium atom in **2(SDiazMesSe)•5(IF₅B)**. The

length of these halogen bonds (I···Se = 3.2808(5) Å and 3.3211(7) Å) are comparable to the analogous distance in the reported cocrystal of IF₅B and 1,1-dimethylselenourea (I···Se = 3.2841(12) Å) (Chernysheva *et al.*, 2021). The halogen bonds are similar when normalized for the increased van der Waals radius of selenium versus sulfur. The packing is consolidated along the *a* axis through weak $C-F\cdots\pi$ interactions.

Figure 8 Halogen bonding in (**SDiazMesS**)•(**IF**₅**B**) and **2**(**SDiazMesSe**)•5(**IF**₅**B**). Intermolecular I···S and I···Se halogen bonding is indicated by magenta dotted lines. Displacement ellipsoids are drawn at the 50% probability level. Hydrogen atoms are omitted for clarity.

3.5. Cocrystallization of SDiazMesS and SDiazMesSe with tetraiodoethylene

The final pair of cocrystals, **2(SDiazMesS)•(TIE)** and **2(SDiazMesSe)•(TIE)**, are both obtained in the triclinic space group *P*-1, with one thione of selone molecule and one half of a TIE molecule per asymmetric unit. A single halogen bond is observed to the chalcogen atom, contributing to discrete 2:1 units within the structure. The remaining two iodine atoms of each TIE molecule appear to be pinned in place by weak C-H---I interactions from methyl groups of three neighboring SDiazMesE molecules, contributing to the formation of ribbons in the *bc* plane.

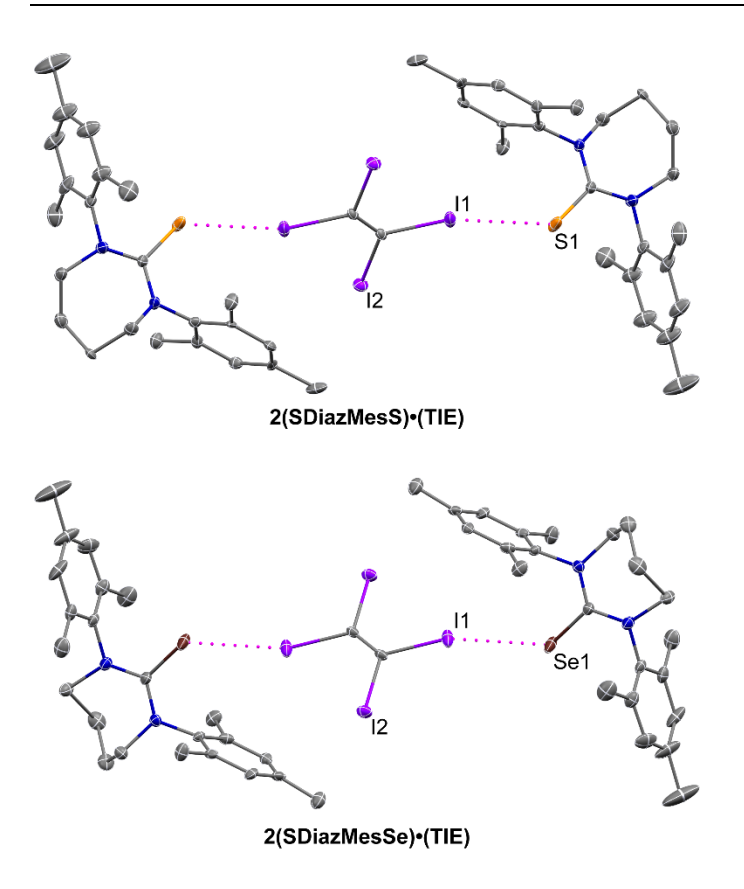


Figure 9 Halogen bonding in the TIE containing cocrystals. Intermolecular I···S and I···Se halogen bonding is indicated by magenta dotted lines. Displacement ellipsoids are drawn at the 50% probability level. Hydrogen atoms are omitted for clarity.

4. Conclusions

The heterocyclic molecules hexahydro-1,3-bis(2,4,6-trimethylphenyl)-2H-1,3-diazepine-2-thione and hexahydro-1,3-bis(2,4,6-trimethylphenyl)-2H-1,3-diazepine-2-selone provided a robust template for halogen and/or chalcogen bonding interactions, yielding a total of 24 new cocrystal structures. The reaction with molecule diiodine provided products incorporating S–I–I and Se–I–I fragments with a wide range of bond orders. When this reaction was conducted in acetone, oxidative addition of acetone to the chalcogen atom allowed the formation of new C–S, C–Se, and C–C covalent bonds under mild conditions. Cocrystallization with iodopentafluorobenzene, 1,2-, 1,3-, and 1,4-diiodotetrafluorobenzene, 1,3,5-trifluorotriiodobenzene, and tetraiodoethylene reveals structures that, in most cases, show a preference for halogen over chalcogen bonding and are typically isomorphic. This series of structural data supports the power of crystallographic study to reveal unexpected and unique interactions and reaction pathways.

Table 1 Selected bond lengths in **SDiazMesE**, (**SDiazMesE**)•(MeCN), and the products of reaction with I_2 (E = S, Se, Å)

Compound	$d_{\mathrm{C=E}}$	$d_{\mathrm{C-N}}$	E–I	I–I

SDiazMesS	1.6887(13)	1.3625(16)	1.361(2)	_	_
CD:amMagCa	1.851(2)	1.361(3)	1.348(3)	_	
SDiazMesSe	1.850(2)	1.356(3)	1.353(3)	_	
(SDiazMesS)•(MeCN)	1.6821(15)	1.3627(17)	1.3689(15)	_	
(SDiazMesSe)•(MeCN)	1.8498(18)	1.355(2)	1.3586(19)	_	
SDiazMesS-I ₂	1.738(3)	1.356(4)	1.337(5)	2.6738(9)	2.8794(4)
SDiazMesSe-I ₂	1.8973(16)	1.334(3)	1.351(2)	2.7559(4)	2.9106(4)
(SDiazMesS–I ₂)•(I ₂)	1.7555(18)	1.335(3)	1.344(2)	2.5052(5)	3.0803(4)
[(SDiazMesSe-I)(I ₃)]	1.921(10)	1.338(13)	1.339(13)	2.5807(14)	3.2052(10)
[(SDiazMesSe–I)(I ₃)]•(DCM)	1.9274(17)	1.331(3)	1.338(3)	2.5958(3)	3.1867(3)
$[(SDiazMesSe-DMK)(I_3)] \bullet (I_2)$	1.910(9)	1.320(12)	1.336(11)	_	
[(SDiazMesS-MIBK)(I ₃)]	1.772(4)	1.339(4)	1.329(4)	_	_
[(SDiazMesSe-MIBK)(I ₃)]	1.9284(17)	1.340(3)	1.328(2)	_	_

 $\textbf{Table 2} \quad \text{Halogen bond geometries in organoiodine-containing cocrystals (Å, °)}$

Compound		$d_{ ext{I}\cdots ext{E}}$	$R_{\mathrm{XB}}^{\mathrm{i}}$	$ heta_{ ext{C-I}\cdots ext{E}}$	<i>Ө</i> с=Е…I	$\theta_1 - \theta_2^{\mathrm{ii}}$
(SDiazMesS)•(1,2-F ₄ DIB)	I1···S1	3.2092(12)	0.85	173.36(13)	129.75(16)	43.6(3)
(SDiazMesS)•(1,3-F ₄ DIB)	I1···S1	3.2795(15)	0.87	170.80(15)	120.09(19)	50.7(3)
(SDIAZINIESS)*(1,5-F4DID)	I2···S1	3.3176(15)	0.88	170.23(15)	133.2(2)	37.0(4)
(SDiagMagSa)a(1.2 E.DID)	I1···Se1	3.3348(5)	0.86	170.03(10)	115.89(12)	54.1(2)
(SDiazMesSe)•(1,3-F ₄ DIB)	I2···Se1	3.3550(7)	0.87	166.71(10)	131.03(12)	35.7(2)
2(SDiazMesS)•(1,3-F ₄ DIB)	I1···S1	3.3131(11)	0.88	167.09(8)	123.63(10)	43.46(18)
2(SDiazMesSe)•(1,3-F ₄ DIB)	I1···Se1	3.3280(11)	0.86	168.37(10)	119.78(11)	48.5(2)
(SDiazMesS)•(1,4-F ₄ DIB) ^t	I1···S1	3.2318(7)	0.85	175.67(9)	123.21(9)	52.46(18)
(SDiazMesS)•(1,4-F4DIB) ^m	I1···S1	3.4491(5)	0.91	143.57(6)	131.44(8)	12.13(14)
(SDiazMesSe)•(1,4-F4DIB) ^t	I1···Se1	3.2553(3)	0.84	173.97(4)	120.80(4)	53.17(8)
	I1···S1	3.434(2)	0.91	156.0(3)	127.8(3)	28.2(3)
(SDiazMesS)•(1,3,5-F ₃ I ₃ B)	I4···S1	3.236(2)	0.86	175.8(2)	127.1(3)	48.7(5)
	I5…S2	3.213(2)	0.85	175.9(2)	111.6(3)	64.3(5)

	I7…S2	3.445(2)	0.91	165.5(2)	121.5(3)	44.0(5)
	I3…S3	3.369(2)	0.89	170.7(2)	110.9(3)	59.8(5)
	I9…S2	3.4317(19)	0.91	171.7(3)	118.5(3)	53.2(6)
	I1···Se1	3.5635(5)	0.92	164.91(12)	110.50(12)	54.4(2)
(SDiazMesSe)•(1,3,5-F ₃ I ₃ B)	I2···Se1	3.4758(5)	0.90	170.07(11)	116.97(12)	53.1(2)
	I3···Se1	3.9070(8)	1.01	176.73(10)	131.29(11)	45.4(2)
(SDiazMesS)•(IF5B)	I1···S1	3.1809(14)	0.84	173.11(13)	131.18(16)	41.9(3)
2(SDiazMesSe)•5(IF ₅ B)	I1···Se1	3.2808(5)	0.85	175.12(8)	108.01(6)	67.11(14)
	I2···Se1	3.3211(7)	0.86	170.52(7)	129.54(9)	40.98(16)
2(SDiazMesS)•(TIE)	I1···S1	3.1969(13)	0.85	164.79(11)	131.12(11)	33.7(2)
2(SDiazMesSe)•(TIE)	I1···Se1	3.2139(4)	0.83	162.73(15)	129.35(8)	33.4(2)

(i) $R_{XB} = d_{X\cdots Y}/\sum d_{Vdw}$, the ratio of the distance between the donor atom (i.e., I) and the acceptor atom (i.e., S, Se) to the sum of their van der Waals radii (S, 1.80 Å; Se, 1.90 Å; I, 1.98 Å). (ii) $\theta_1 - \theta_2 = |[(\theta_{C-I\cdots E}) - (\theta_{C=E\cdots I})]|$

 Table 3
 Experimental details

Table 4	(SDiazMesS)	(SDiazMesSe)	(SDiazMesS_MeCN)	(SDiazMesSe_MeCN)
Crystal data				
Chemical formula	$C_{23}H_{30}N_2S$	$C_{23}H_{30}N_2Se$	$C_{23}H_{30}N_{2}S\!\cdot\!C_{2}H_{3}N$	$C_{23}H_{30}N_2Se\cdot C_2H_3N$
$M_{ m r}$	366.55	413.45	407.60	454.50
Crystal system, space group	Monoclinic, $P2_1/c$	Orthorhombic, Pbca	Monoclinic, $P2_1/c$	Monoclinic, $P2_1/c$
Temperature (K)	100	100	100	100
a, b, c (Å)	16.4064 (14), 8.7386 (9), 14.8229 (14)	17.4279 (4), 15.2522 (4), 31.0253 (7)	13.0884 (6), 12.9760 (5), 14.4293 (7)	13.1365 (3), 13.3024 (2), 14.2478 (3)
α, β, γ (°)	90, 104.983 (3), 90	90, 90, 90	90, 113.028 (2), 90	90, 113.1557 (7), 90
$V(Å^3)$	2052.9 (3)	8247.0 (3)	2255.32 (18)	2289.18 (8)

Z	4	16	4	4
Radiation type	Μο Κα	Μο Κα	Μο Κα	Μο Κα
$\mu \ (mm^{-1})$	0.17	1.83	0.16	1.66
Crystal size (mm)	$0.30 \times 0.19 \times 0.17$	$0.08 \times 0.07 \times 0.07$	$0.26 \times 0.17 \times 0.10$	$0.23 \times 0.19 \times 0.10$
Data collection				
Diffractometer	Bruker D8 Venture Photon 2		Bruker D8 Venture Photon 2	Bruker D8 Venture Photon 2
Absorption correction	Multi-scan SADABS v2016/2 (Bruker AXS Inc., 2017)	Multi-scan SADABS v2016/2 (Bruker AXS Inc., 2017)	Multi-scan SADABS v2016/2 (Bruker AXS Inc., 2017)	Multi-scan SADABS v2016/2 (Bruker AXS Inc., 2017)
$T_{ m min},T_{ m max}$	0.706, 0.746	0.697, 0.746	0.711, 0.746	0.683, 0.746
No. of measured, independent and observed [$I > 2\sigma(I)$] reflections	33473, 4240, 3717	72880, 9109, 7294	34671, 5148, 4419	40871, 5251, 4637
$R_{ m int}$	0.044	0.072	0.046	0.046
$(\sin\theta/\lambda)_{max}(\mathring{A}^{-1})$	0.628	0.642	0.649	0.650
Refinement				
$R[F^2 > 2\sigma(F^2)],$ $wR(F^2), S$	0.037, 0.097, 1.03	0.036, 0.078, 1.03	0.038, 0.096, 1.06	0.026, 0.061, 1.08
No. of reflections	4240	9109	5148	5251
No. of parameters	241	481	288	288
No. of restraints	0	0	36	36
H-atom treatment	H-atom parameters constrained	H-atom parameters constrained	H-atom parameters constrained	H-atom parameters constrained
			$w = 1/[\sigma^{2}(F_{o}^{2}) + (0.0294P)^{2} + 1.5344P]$ where $P = (F_{o}^{2} + 2F_{c}^{2})/3$	$(0.0125P)^2 + 1.9573P$

	where $P = (F_0^2 + 2F_c^2)/3$	where $P = (F_o^2 + 2F_c^2)/3$		
$\Delta ho_{max}, \Delta ho_{min} (e \ \ \mathring{A}^{-3})$	0.37, -0.27	0.39, -0.33	0.28, -0.21	0.36, -0.33
Absolute structure	; -	-	-	-
Absolute structure parameter	; -	_	-	-
	(SDiazMesSI2)	(SDiazMesSeI2)	(SDiazMesSI2_I2)	(SDiazMesSeI_I3)
Crystal data				
Chemical formula	$C_{23}H_{30}I_{2}N_{2}S$	$C_{23}H_{30}I_2N_2Se$	$2(C_{23}H_{30}I_2N_2S)\cdot 2(I_2)$	$C_{23}H_{30}IN_2Se\cdot I_3$
$M_{ m r}$	620.35	667.25	1748.30	921.05
Crystal system, space group	Triclinic, P-1	Triclinic, P-1	Triclinic, P-1	Monoclinic, $P2_1/n$
Temperature (K)	100	100	100	100
<i>a</i> , <i>b</i> , <i>c</i> (Å)	7.9505 (4), 8.5048 (4), 18.2812 (9)	8.0282 (6), 8.4305 (8), 18.3525 (16)	8.3022 (9), 11.3510 (11), 15.5656 (16)	11.0063 (7), 22.9632 (14), 11.1015 (6)
α, β, γ (°)	81.040 (3), 89.926 (2), 85.125 (2)	81.814 (4), 89.706 (4), 85.171 (4)	83.691 (4), 87.180 (4) 75.024 (4)	90, 93.024 (2), 90
$V(Å^3)$	1216.54 (10)	1225.08 (18)	1408.1 (3)	2801.9 (3)
Z	2	2	1	4
Radiation type	Μο Κα	Μο Κα	Μο Κα	Μο Κα
$\mu (mm^{-1})$	2.68	4.06	4.51	5.76
Crystal size (mm)	$0.17 \times 0.12 \times 0.08$	$0.19 \times 0.15 \times 0.13$	$0.19 \times 0.09 \times 0.04$	$0.06\times0.06\times0.02$
Data collection				
Diffractometer	Bruker D8 Venture Photon 2	Bruker D8 Venture Photon 2	Bruker D8 Venture Photon 2	Bruker D8 Venture Photon 2
Absorption correction	Multi-scan SADABS v2016/2	Multi-scan SADABS v2016/2	Multi-scan SADABS v2016/2	Multi-scan SADABS v2016/2

	(Bruker AXS Inc., 2017)	(Bruker AXS Inc., 2017)	(Bruker AXS Inc., 2017)	(Bruker AXS Inc., 2017)
T_{\min}, T_{\max}	0.636, 0.746	0.634, 0.746	0.579, 0.746	0.606, 0.746
No. of measured, independent and observed $[I > 2\sigma(I)]$ reflections	37544, 5455, 4834	53696, 7479, 6504	71058, 8260, 7603	36709, 6428, 5536
$R_{ m int}$	0.067	0.045	0.035	0.091
$(\sin\theta/\lambda)_{max}(\mathring{A}^{-1})$	0.646	0.715	0.706	0.650
Refinement				
$R[F^2 > 2\sigma(F^2)],$ $wR(F^2), S$	0.034, 0.072, 1.12	0.023, 0.049, 1.10	0.017, 0.039, 1.18	0.062, 0.127, 1.17
No. of reflections	5455	7479	8260	6428
No. of parameters	259	259	277	278
No. of restraints	0	0	0	30
H-atom treatment	H-atom parameters constrained	H-atom parameters constrained	H-atom parameters constrained	H-atom parameters constrained
	$w = 1/[\sigma^{2}(F_{o}^{2}) + (0.0141P)^{2} + 2.7069P]$ where $P = (F_{o}^{2} + 2F_{c}^{2})/3$	2 ()	$w = 1/[\sigma^{2}(F_{o}^{2}) + (0.0082P)^{2} + 1.3172P]$ where $P = (F_{o}^{2} + 2F_{c}^{2})/3$	$(0.0131P)^2 +$
$\Delta ho_{max}, \Delta ho_{min}$ (e \mathring{A}^{-3})	1.35, -1.40	0.70, -0.75	0.50, -0.74	2.17, -1.40
Absolute structure	; -	-	-	-
Absolute structure parameter	· -	-	-	-

Crystal data				
Chemical formula	$C_{23}H_{30}IN_2Se\cdot I_3\cdot CH_2Cl_2$	$3.333(I_{1.5}) \cdot C_{26}H_{35}N_2OSe$	I ₃ ·C ₂₉ H ₄₁ N ₂ OS	$I_3 \cdot C_{29} H_{41} N_2 OSe$
$M_{ m r}$	1005.97	1105.02	846.40	893.30
Crystal system, space group	Triclinic, <i>P</i> -1	Monoclinic, C2/c	Triclinic, P-1	Triclinic, P-1
Temperature (K)	100	100	100	100
a,b,c (Å)	8.4541 (4), 8.5353 (4), 22.0045 (11)	13.2501 (6), 11.0708 (6), 45.509 (3)	8.7838 (8), 14.2194 (15), 15.1418 (15)	8.8091 (5), 14.2584 (8), 15.1228 (9)
α, β, γ (°)	93.258 (2), 90.198 (2), 98.032 (2)	90, 96.722 (2), 90	63.522 (3), 74.494 (4), 80.494 (4)	63.952 (2), 74.061 (2), 81.113 (2)
$V(\mathring{\mathbf{A}}^3)$	1569.58 (13)	6629.7 (6)	1628.9 (3)	1639.67 (17)
Z	2	8	2	2
Radiation type	Μο Κα	Μο Κα	Μο Κα	Μο Κα
$\mu \text{ (mm}^{-1}\text{)}$	5.32	5.81	2.97	3.99
Crystal size (mm)	$0.24 \times 0.15 \times 0.05$	$0.17 \times 0.15 \times 0.05$	$0.11 \times 0.09 \times 0.08$	$0.17 \times 0.11 \times 0.08$
Data collection	on			
Diffractometer	e Bruker D8 Venture Photon 2	Bruker D8 Venture Photon 2	Bruker D8 Venture Photon 2	Bruker D8 Venture Photon 2
Absorption correction	Multi-scan SADABS v2016/2 (Bruker AXS Inc., 2017)	Multi-scan SADABS v2016/2 (Bruker AXS Inc., 2017)	Multi-scan SADABS v2016/2 (Bruker AXS Inc., 2017)	Multi-scan SADABS v2016/2 (Bruker AXS Inc., 2017)
T_{\min}, T_{\max}	0.527, 0.746	0.561, 0.745	0.645, 0.746	0.640, 0.746
No. of measured, independent	64752, 8821, 7994	46614, 6580, 5737	60178, 8827, 6624	75078, 9229, 7989

and observed $[I > 2\sigma(I)]$ reflections				
R_{int}	0.038	0.041	0.052	0.041
$(\sin \theta/\lambda)_{max}$ (\mathring{A}^{-1})	0.695	0.620	0.687	0.696
Refinement				
$R[F^2 > 2\sigma(F^2)],$ $wR(F^2), S$	0.019, 0.043, 1.13	0.067, 0.142, 1.10	0.033, 0.069, 1.20	0.024, 0.052, 1.14
No. of reflections	8821	6580	8827	9229
No. of parameters	304	325	333	333
No. of restraints	0	0	0	0
H-atom treatment	H-atom parameters constrained	H-atom parameters constrained	H-atom parameters constrained	H-atom parameters constrained
		$w = 1/[\sigma^{2}(F_{o}^{2}) + (0.018P)^{2} + 376.8008P]$ where $P = (F_{o}^{2} + 2F_{c}^{2})/3$	-	$w = 1/[\sigma^{2}(F_{o}^{2}) + (0.0083P)^{2} + 2.5037P]$ where $P = (F_{o}^{2} + 2F_{c}^{2})/3$
$\Delta \rho_{\text{max}}$, $\Delta \rho_{\text{min}}$ (e Å ⁻³)	0.81, -0.88	4.07, -3.13	2.75, -0.92	1.18, -1.66
Absolute structure	-?	-	-	-
Absolute structure parameter	-	-	-	-

 $(SDiazMesS_12F4DI \quad (SDiazMesS_13F4DI \quad (SDiazMesSe_13F4DI \quad (2SDiazMesS_13F4DI \quad (2SDiazMe$

	B)	B)	В)	B)
Crystal data				
Chemical formula	$C_6F_4I_2 \cdot C_{23}H_{30}N_2S$	$C_{6}F_{4}I_{2}\cdot C_{23}H_{30}N_{2}S$	$C_6F_4I_2\cdot C_{23}H_{30}N_2Se$	C ₆ F ₄ I ₂ ·2(C ₂₃ H ₃₀ N ₂ S)
$M_{ m r}$	768.41	768.41	815.31	1134.96
Crystal system, space group	Orthorhombic, Pna2 ₁	Orthorhombic, $P2_12_12_1$	Orthorhombic, $P2_12_12_1$	Monoclinic, C2/c
Temperature (K)	100	100	100	100
a,b,c (Å)	7.6668 (5), 16.8546 (11), 22.3786 (15)	8.2080 (2), 12.9974 (2), 27.2463 (5)	8.2583 (2), 12.9953 (4), 27.2240 (7)	39.0981 (14), 17.0474 (6), 7.3957 (2)
$\alpha,\beta,\gamma(^\circ)$	90, 90, 90	90, 90, 90	90, 90, 90	90, 94.344 (1), 90
$V(Å^3)$	2891.8 (3)	2906.71 (10)	2921.66 (14)	4915.2 (3)
Z	4	4	4	4
Radiation type	Μο Κα	Μο Κα	Μο Κα	Μο Κα
$\mu \ (mm^{-1})$	2.30	2.28	3.45	1.42
Crystal size (mm)	$0.22 \times 0.07 \times 0.07$	$0.15 \times 0.14 \times 0.06$	$0.29 \times 0.08 \times 0.07$	$0.28 \times 0.09 \times 0.03$
Data collection	n			
Diffractomete r	Bruker D8 Venture Photon 2	Bruker D8 Venture Photon 2	Bruker D8 Venture Photon 2	Bruker D8 Venture Photon 2
Absorption correction	Multi-scan SADABS v2016/2 (Bruker AXS Inc., 2017)	Multi-scan SADABS v2016/2 (Bruker AXS Inc., 2017)	Multi-scan SADABS v2016/2 (Bruker AXS Inc., 2017)	Multi-scan SADABS v2016/2 (Bruker AXS Inc., 2017)
T_{\min} , T_{\max}	0.621, 0.746	0.676, 0.746	0.494, 0.746	0.663, 0.746
No. of measured, independent	50096, 7186, 6786	28002, 6938, 6327	85940, 7878, 7491	40822, 5102, 4240

and observed $[I > 2\sigma(I)]$ reflections				
$R_{ m int}$	0.044	0.048	0.047	0.060
$(\sin\theta/\lambda)_{max}$ (\mathring{A}^{-1})	0.668	0.658	0.686	0.628
Refinement				
$R[F^2 > 2\sigma(F^2)],$ $wR(F^2), S$	0.025, 0.058, 1.10	0.031, 0.065, 1.09	0.022, 0.044, 1.13	0.029, 0.061, 1.16
No. of reflections	7186	6938	7878	5102
No. of parameters	349	386	386	334
No. of restraints	1	96	96	0
H-atom treatment	H-atom parameters constrained	H-atom parameters constrained	H-atom parameters constrained	H-atom parameters constrained
	- ` `	$w = 1/[\sigma^2(F_o^2) + 4.5084P]$ where $P = (F_o^2 + 2F_c^2)/3$	$w = 1/[\sigma^{2}(F_{o}^{2}) + (0.003P)^{2} + 3.3501P]$ where $P = (F_{o}^{2} + 2F_{c}^{2})/3$	- ` ´
$\Delta \rho_{\text{max}}, \Delta \rho_{\text{min}}$ (e Å ⁻³)	0.77, -0.70	1.19, -1.17	0.99, -0.93	1.02, -0.53
Absolute structure	Flack x determined using 3124 quotients [(I+)-(I-)]/[(I+)+(I-)] (Parsons, Flack and Wagner, Acta Cryst. B69 (2013) 249-259).	Flack x determined using 2576 quotients [(I+)-(I-)]/[(I+)+(I-)] (Parsons, Flack and Wagner, Acta Cryst. B69 (2013) 249-259).	Flack x determined using 3173 quotients [(I+)-(I-)]/[(I+)+(I-)] (Parsons, Flack and Wagner, Acta Cryst. B69 (2013) 249-259).	-
Absolute structure	-0.025 (7)	-0.034 (12)	0.003 (4)	-

parameter

	(2SDiazMesSe_13F4 DIB)	(2SDiazMesS_14F4DI B_t)	(2SDiazMesSe_14F4DI B_t)	(2SDiazMesS_14F4DIB _m)
Crystal data				
Chemical formula	$C_6F_4I_2 \cdot 2(C_{23}H_{30}N_2Se)$	$C_6F_4I_2 \cdot 2(C_{23}H_{30}N_2S)$	$C_6F_4I_2 \cdot 2(C_{23}H_{30}N_2Se)$	$C_6F_4I_2 \cdot 2(C_{23}H_{30}N_2S)$
$M_{ m r}$	1228.76	1134.96	1228.76	1134.96
Crystal system, space group	Monoclinic, C2/c	Triclinic, P-1	Triclinic, P-1	Monoclinic, $P2_1/c$
Temperature (K)	: 100	100	100	100
<i>a</i> , <i>b</i> , <i>c</i> (Å)	39.058 (4), 17.2429 (14), 7.4287 (6)	7.5020 (7), 12.2475 (11), 14.4780 (13)	7.5969 (4), 12.1995 (7), 14.4439 (8)	13.3377 (6), 15.2129 (6), 13.0613 (5)
α, β, γ (°)	90, 94.012 (4), 90	104.905 (3), 95.822 (3), 104.609 (3)	104.6128 (18), 95.7464 (19), 104.1188 (18)	90, 109.998 (1), 90
$V(Å^3)$	4990.8 (7)	1224.10 (19)	1237.42 (12)	2490.41 (18)
Z	4	1	1	2
Radiation type	Μο Κα	Μο Κα	Μο Κα	Μο Κα
$\mu \; (mm^{-1})$	2.77	1.43	2.80	1.40
Crystal size (mm)	$0.39 \times 0.04 \times 0.04$	$0.18 \times 0.04 \times 0.04$	$0.21 \times 0.17 \times 0.10$	$0.18 \times 0.16 \times 0.06$
Data collecti	ion			
Diffractomer	t Bruker D8 Venture Photon 2	Bruker D8 Venture Photon 2	Bruker D8 Venture Photon 2	Bruker D8 Venture Photon 2
Absorption correction	Multi-scan SADABS v2016/2 (Bruker AXS Inc., 2017)			

	2017)	2017)	2017)	
$T_{ m min},T_{ m max}$	0.623, 0.745	0.679, 0.746	0.582, 0.746	0.683, 0.746
No. of measured, independent and observed [$I > 2\sigma(I)$] reflections	52044, 4907, 4119	16839, 5058, 4439	42081, 7215, 6861	53110, 5713, 5146
$R_{ m int}$	0.068	0.045	0.031	0.042
$(\sin\theta/\lambda)_{max}$ (\mathring{A}^{-1})	0.617	0.628	0.705	0.650
Refinement				
$R[F^2 > 2\sigma(F^2)],$ $wR(F^2), S$	0.031, 0.068, 1.24	0.030, 0.060, 1.13	0.017, 0.041, 1.07	0.024, 0.056, 1.10
No. of reflections	4907	5058	7215	5713
No. of parameters	297	295	295	295
No. of restraints	0	0	0	0
H-atom treatment	H-atom parameters constrained	H-atom parameters constrained	H-atom parameters constrained	H-atom parameters constrained
	$w = 1/[\sigma^2(F_o^2) +$ $28.6286P]$ where $P = (F_o^2 +$ $2F_c^2)/3$	- ` ′	$w = 1/[\sigma^{2}(F_{o}^{2}) + (0.0149P)^{2} + 0.707P]$ where $P = (F_{o}^{2} + 2F_{c}^{2})/3$	[- (- 0)
$\Delta \rho_{\text{max}}, \Delta \rho_{\text{min}}$ (e Å ⁻³)	1.00, -0.67	1.15, -0.66	0.44, -0.51	1.26, -1.41
Absolute structure	-	-	-	-

Absolute - structure parameter	-	-		-
	(SDiazMesS_135F3I3B)) (SDiazMesSe_135F3I3B)	(SDiazMesS_IF5B)	(2SDiazMesSe_5F5IB)
Crystal data				
Chemical formula	3(C ₆ F ₃ I ₃)·3(C ₂₃ H ₃₀ N ₂ S)	$C_6F_3I_3 \cdot C_{23}H_{30}N_2Se$	$C_6F_5I\cdot C_{23}H_{30}N_2S$	$5(C_6F_5I)\cdot 2(C_{23}H_{30}N_2Se)$
$M_{ m r}$	2628.92	923.21	660.51	2296.70
Crystal system, space group	Monoclinic, $P2_1/c$	Monoclinic, $P2_1/n$	Orthorhombic, Pna2 ₁	Monoclinic, $P2_1/c$
Temperature (K)	100	100	100	100
<i>a</i> , <i>b</i> , <i>c</i> (Å)	39.226 (4), 7.9811 (9), 30.341 (4)	8.0412 (6), 30.070 (2), 12.4774 (10)	7.8472 (5), 16.1751 (13), 21.7956 (19)	25.9292 (14), 8.0709 (4), 20.4309 (11)
$\alpha,\beta,\gamma\;(^\circ)$	90, 106.162 (4), 90	90, 92.632 (3), 90	90, 90, 90	90, 113.037 (2), 90
$V(Å^3)$	9123.3 (18)	3013.8 (4)	2766.5 (4)	3934.6 (4)
Z	4	4	4	2
Radiation type	· Μο <i>Κ</i> α	Μο Κα	Μο Κα	Μο Κα
$\mu \; (mm^{-1})$	3.19	4.36	1.29	3.01
Crystal size (mm)	$0.34 \times 0.05 \times 0.05$	$0.19 \times 0.06 \times 0.05$	$0.41 \times 0.06 \times 0.03$	$0.24 \times 0.19 \times 0.13$
Data collection	1			
Diffractometer	r Bruker D8 Venture Photon 2	Bruker D8 Venture Photon 2	Bruker D8 Venture Photon 2	Bruker D8 Venture Photon 2
Absorption correction	Multi-scan SADABS v2016/2 (Bruker AXS Inc., 2017)	Multi-scan SADABS v2016/2 (Bruker AXS Inc., 2017)	Multi-scan SADABS v2016/2 (Bruker AXS Inc., 2017)	Multi-scan SADABS v2016/2 (Bruker AXS Inc., 2017)

$T_{ m min},T_{ m max}$	0.625, 0.745	0.617, 0.746	0.632, 0.746	0.662, 0.746
No. of measured, independent and observed $[I > 2\sigma(I)]$ reflections	105324, 17944, 15994	42494, 6919, 5611	30210, 6227, 5489	61094, 9058, 8222
$R_{ m int}$	0.054	0.058	0.048	0.035
$(\sin \theta/\lambda)_{max}$ (\mathring{A}^{-1})	0.618	0.650	0.652	0.650
Refinement				
$R[F^2 > 2\sigma(F^2)],$ $wR(F^2), S$	0.053, 0.117, 1.27	0.031, 0.064, 1.17	0.028, 0.063, 1.12	0.024, 0.053, 1.09
No. of reflections	17944	6919	6227	9058
No. of parameters	1064	349	349	565
No. of restraints	36	0	1	51
H-atom treatment	H-atom parameters constrained	H-atom parameters constrained	H-atom parameters constrained	H-atom parameters constrained
	146.2483 <i>P</i>]	$w = 1/[\sigma^{2}(F_{o}^{2}) + (0.0047P)^{2} + 7.9038P]$ where $P = (F_{o}^{2} + 2F_{c}^{2})/3$	$(0.0101P)^2 +$	$(0.0103P)^2 + 7.6201P$] where $P = (F_0^2 +$
$\Delta ho_{ m max}, \Delta ho_{ m min}$ ($ ho^{-3}$)	e 1.36, -1.13	0.78, -0.75	0.68, -0.52	1.06, -0.75
Absolute structure	-	-	Flack x determined using 2370 quotients [(I+)-(I-	-

Absolute - structure parameter	(0 V C 2	Parsons, Flack and Vagner, Acta Pryst. B69 (2013) 49-259).
	(2SDiazMesS_TIE)	(2SDiazMesSe_TIE)
Crystal data		
Chemical formula	$CI_2 \cdot C_{23}H_{30}N_2S$	$C_2I_4 \cdot 2(C_{23}H_{30}N_2Se)$
$M_{ m r}$	632.36	1358.52
Crystal system, space group	Triclinic, P-1	Triclinic, P-1
Temperature (K)	100	100
a, b, c (Å)	7.9170 (6), 11.6457 (8), 15.0306 (10)	7.9777 (5), 11.7334 (7), 15.0059 (9)
α, β, γ (°)	67.358 (2), 83.953 (2), 72.067 (2)	67.540 (2), 82.671 (2), 71.632 (2)
$V(Å^3)$	1216.73 (15)	1231.91 (13)
Z	2	1
Radiation type	Μο Κα	Μο Κα
μ (mm ⁻¹)	2.68	4.04
Crystal size (mm)	$0.23 \times 0.13 \times 0.05$	$0.14 \times 0.09 \times 0.08$
Data collection		
Diffractometer	Bruker D8 Venture Photon 2	Bruker D8 Venture Photon 2
Absorption correction	Multi-scan SADABS v2016/2 (Bruker AXS Inc., 2017)	Multi-scan SADABS v2016/2 (Bruker AXS Inc., 2017)
$T_{ m min},~T_{ m max}$	0.598, 0.746	0.636, 0.746
No. of measured, independent	38610, 6789, 6164	41652, 6224, 5668

and

observed $[I > 2\sigma(I)]$ reflections

 R_{int} 0.038 0.037

 $(\sin \theta/\lambda)_{\text{max}} (\mathring{A}^{-1})$ 0.696 0.671

Refinement

 $R[F^2 > 2\sigma(F^2)], wR(F^2), S$ 0.032, 0.070, 1.06 0.030, 0.065, 1.08

No. of reflections 6789 6224

No. of parameters 384 384

No. of restraints 30 36

H-atom treatment H-atom parameters constrained H-atom parameters constrained

 $w = 1/[\sigma^2(F_o^2) + 5.6607P]$ $w = 1/[\sigma^2(F_o^2) + 5.9779P]$ where $P = (F_o^2 + 2F_c^2)/3$ where $P = (F_o^2 + 2F_c^2)/3$

 $\Delta \rho_{\text{max}}, \Delta \rho_{\text{min}}$ (e Å⁻³) 3.79, -3.62 3.78, -3.88

Absolute structure - -

Absolute structure parameter - -

Computer programs: *APEX3* v2017.3-0 (Bruker AXS Inc., 2017), *SAINT* V8.38A (Bruker AXS Inc., 2017), SHELXT 2018/2 (Sheldrick, 2015a), *SHELXL* 2018/3 (Sheldrick, 2015b), *Mercury* (Macrae *et al.*, 2008), Olex2 1.5 (Dolomanov *et al.*, 2009).

Table 5 Hydrogen-bond geometry (Å, °) for (SDiazMesS)

 D— $H \cdots A$ D—H $H \cdots A$ $D \cdots A$ D— $H \cdots A$

 C3— $H3B \cdots S1^i$ 0.99 3.01 3.7030 (15) 128

 C5— $H5A \cdots S1^i$ 0.99 2.87 3.4858 (14) 121

Symmetry code: (i) x, -y+3/2, z+1/2.

Table 6 Hydrogen-bond geometry (Å, °) for (SDiazMesSe)

 D—H···A
 D—H···A
 D—H···A

 C2—H2B···Se1ⁱ
 0.99
 3.02
 3.671 (2)
 125

C3—H3A···Se1 ⁱ	0.99	2.88	3.665 (2)	137
C4—H4B····Se2 ⁱⁱ	0.99	3.12	3.641 (2)	114
C5—H5A····Se2 ⁱⁱ	0.99	3.09	3.754 (2)	126
C26—H26B····Se2 ⁱⁱⁱ	0.99	2.94	3.796 (2)	146

Symmetry codes: (i) -x+1/2, y+1/2, z; (ii) -x+1, -y+1, -z+1; (iii) -x+1/2, y-1/2, z.

Table 7 Hydrogen-bond geometry (Å, °) for (SDiazMesS MeCN)

D — $H \cdots A$	<i>D</i> —H	$H\cdots A$	$D \cdots A$	D — $H \cdots A$
C4—H4 <i>B</i> ····S1 ⁱ	0.99	2.92	3.6972 (17)	136
C25—H25 <i>B</i> ····S1 ⁱⁱ	0.98	2.92	3.8180 (17)	152

Symmetry codes: (i) -x+1, y-1/2, -z+3/2; (ii) -x+1, -y+1, -z+1.

Table 8 Hydrogen-bond geometry (Å, °) for (SDiazMesSe_MeCN)

D— H ··· A	<i>D</i> —H	$H\cdots A$	$D\cdots A$	<i>D</i> —H··· <i>A</i>
C4—H4A···Se1 ⁱ	0.99	3.09	4.009 (6)	155
C4—H4B···Se1 ⁱⁱ	0.99	2.91	3.737 (4)	141
C4 <i>B</i> —H4 <i>BB</i> ···Se1 ⁱⁱ	0.99	3.15	3.965 (3)	141
C25—H25 <i>B</i> ···Se1 ⁱⁱⁱ	0.98	3.03	3.829 (2)	140

Symmetry codes: (i) x, -y+1/2, z+1/2; (ii) -x+1, y-1/2, -z+3/2; (iii) -x+1, -y+1, -z+1.

Table 9 Hydrogen-bond geometry (Å, °) for (SDiazMesSI2)

D — $H \cdots A$	<i>D</i> —H	$H\cdots A$	$D \cdots A$	<i>D</i> —H··· <i>A</i>
C2—H2 <i>B</i> ···I1 ⁱ	0.99	3.16	4.111 (4)	162
C4—H4 <i>B</i> ····I2 ⁱⁱ	0.99	3.16	4.034 (4)	148
C5—H5 <i>A</i> ···I1 ⁱ	0.99	3.10	3.896 (3)	138

Symmetry codes: (i) x+1, y, z; (ii) x+1, y-1, z.

Table 10 Hydrogen-bond geometry (Å, °) for (SDiazMesSeI2)

<i>D</i> —H··· <i>A</i>	<i>D</i> —H	$H\cdots A$	$D \cdots A$	<i>D</i> —H··· <i>A</i>
C2—H2A···I1 ⁱ	0.99	3.08	3.885 (2)	139

Acta Crystallographica Section B	research papers				
C3—H3 <i>B</i> ···I2 ⁱⁱ	0.99	3.14	4.007 (2)	147	
C5—H5 <i>B</i> ···I1 ⁱ	0.99	3.11	4.067 (2)	164	
Symmetry codes: (i) $x+1$, y , z ; (ii) $x+1$, y	−1, z.				
Table 11 Hydrogen-bond geometry (Å, °) for (SDiazMesSI2_I2)					
D — $H\cdots A$	<i>D</i> —Н	$H\cdots A$	$D\cdots A$	D— H ··· A	
C2—H2 <i>B</i> ···I4 ⁱ	0.99	3.22	3.7794 (18)	118	
C5—H5 <i>A</i> ···I2 ⁱⁱ	0.99	3.26	4.0837 (19)	142	
Symmetry codes: (i) $x+1$, y , z ; (ii) $x+1$, y	−1, <i>z</i> .				
Table 12 Hydrogen-bond geometry (Å, °) for (SDiazMesSeI_I3)					
D — $H\cdots A$	<i>D</i> —Н	$H\cdots A$	$D \cdots A$	D— H ··· A	
C2—H2 <i>A</i> ···I3 ⁱ	0.99	3.24	4.029 (10)	138	

C2—H2B··· $I4^{i}$ 0.99 3.12 129 3.823 (11) C3—H3*B*····I2ⁱⁱ 0.99 3.22 3.998 (11) 137 C5—H5B···Se1ⁱⁱⁱ 0.99 3.09 3.693 (11) 121

Symmetry codes: (i) -x+1, -y+1, -z+1; (ii) x-1, y, z; (iii) x-1/2, -y+3/2, z-1/2.

 Table 13
 Hydrogen-bond geometry (Å, °) for (SDiazMesSeI_I3_DCM)

D — $H \cdots A$	<i>D</i> —H	$H\cdots A$	$D \cdots A$	D — $H \cdots A$
C2—H2 <i>B</i> ···I3 ⁱ	0.99	3.24	3.755 (2)	114
C4—H4 <i>A</i> ···I3 ⁱⁱ	0.99	3.15	3.748 (2)	120
C5—H5 <i>A</i> ····I1 ⁱ	0.99	3.09	3.930 (2)	144

Symmetry codes: (i) x-1, y, z; (ii) x-1, y+1, z.

Table 14 Hydrogen-bond geometry (Å, °) for (SDiazMesSeDMK_I3_I2)

D— H ··· A	<i>D</i> —H	$H\cdots A$	$D \cdots A$	D — $H \cdots A$
C2—H2 <i>A</i> ····I2 ⁱ	0.99	3.29	4.274 (10)	173
C3—H3 <i>B</i> ····I2 ⁱⁱ	0.99	3.06	3.674 (14)	122
C4—H4 <i>B</i> ···O1 ⁱⁱⁱ	0.99	2.32	3.081 (13)	133

C26—H26B···I6 iv

0.98

3.26

4.186 (13)

158

Symmetry codes: (i) -x+1, -y+1, -z+1; (ii) x-1/2, y+1/2, z; (iii) x-1/2, y-1/2, z; (iv) x+1/2, y+1/2, z.

Table 15 Hydrogen-bond geometry (Å, °) for (SDiazMesSMIBK_I3)

D — $H\cdots A$	<i>D</i> —H	$H\cdots A$	$D \cdots A$	<i>D</i> —H··· <i>A</i>
C2—H2A···I1	0.99	3.07	3.693 (3)	122
C2—H2 <i>B</i> ···I2	0.99	3.17	3.986 (3)	141

Table 16 Hydrogen-bond geometry (Å, °) for (SDiazMesSeMIBK I3)

D — $H \cdots A$	<i>D</i> —H	$H\cdots A$	$D\cdots A$	<i>D</i> —H··· <i>A</i>
C2—H2 <i>A</i> ···I3	0.99	3.10	3.690 (2)	120
C2—H2 <i>B</i> ···I2	0.99	3.16	4.003 (2)	144
C3—H3 <i>A</i> ···O1 ⁱ	0.99	2.63	3.560 (3)	156

Symmetry code: (i) x+1, y, z.

Table 17 Hydrogen-bond geometry (Å, °) for (SDiazMesS 12F4DIB)

<i>D</i> —H··· <i>A</i>	<i>D</i> —H	$H\cdots A$	$D \cdots A$	<i>D</i> —H··· <i>A</i>
C2—H2 <i>B</i> ····I2 ⁱ	0.99	3.11	4.041 (6)	156
C3—H3 <i>A</i> ···S1 ⁱⁱ	0.99	2.94	3.553 (7)	121

Symmetry codes: (i) -x+1, -y+1, z+1/2; (ii) x-1, y, z.

Table 18 Hydrogen-bond geometry (Å, °) for (SDiazMesS_13F4DIB)

D — $H\cdots A$	<i>D</i> —H	$H\cdots A$	$D \cdots A$	<i>D</i> —H··· <i>A</i>
C2—H2 <i>A</i> ···I2 ⁱ	0.99	3.19	3.897 (12)	129
C5—H5 <i>A</i> ···F4	0.99	2.62	3.330 (11)	129
C2 <i>B</i> —H2 <i>BB</i> ···I1 ⁱⁱ	0.99	3.26	4.115 (12)	146
C4 <i>B</i> —H4 <i>BA</i> ···F3 ⁱⁱⁱ	0.99	2.48	3.247 (13)	134
C5 <i>B</i> —H5 <i>BB</i> ···F4	0.99	2.62	3.153 (12)	114

Symmetry codes: (i) -x+3/2, -y+1, z+1/2; (ii) x+1/2, -y+3/2, -z+1; (iii) x+1/2, -y+1/2, -z+1.

Table 19 Hydrogen-bond geometry (Å, °) for (SDiazMesSe 13F4DIB)

D — $H\cdots A$	<i>D</i> —Н	$H\cdots A$	$D \cdots A$	<i>D</i> —H··· <i>A</i>
C2—H2 <i>B</i> ···I2 ⁱ	0.99	3.22	3.947 (6)	132
C2 <i>B</i> —H2 <i>BA</i> ···I1 ⁱⁱ	0.99	3.28	4.124 (12)	145
C3 <i>B</i> —H3 <i>BA</i> ···Se1 ⁱⁱⁱ	0.99	3.03	3.701 (16)	127
C4 <i>B</i> —H4 <i>BB</i> ···F3 ^{iv}	0.99	2.42	3.214 (13)	137
C5—H5 <i>B</i> ···F4	0.99	2.55	3.299 (6)	132
C5 <i>B</i> —H5 <i>BA</i> ···F4	0.99	2.59	3.119 (11)	114

Symmetry codes: (i) -x+1/2, -y+1, z-1/2; (ii) x-1/2, -y+1/2, -z+1; (iii) x-1, y, z; (iv) x-1/2, -y+3/2, -z+1.

Table 20 Hydrogen-bond geometry (Å, °) for (2SDiazMesS 13F4DIB)

D— H ··· A	<i>D</i> —H	$H\cdots A$	$D \cdots A$	<i>D</i> —H··· <i>A</i>
C5—H5 <i>B</i> ···I1 ⁱ	0.99	3.29	4.117 (5)	143
C3 <i>B</i> —H3 <i>BB</i> ···S1 ⁱ	0.99	2.85	3.574 (9)	131

Symmetry code: (i) x, y, z+1.

Table 21 Hydrogen-bond geometry (Å, °) for (2SDiazMesSe_13F4DIB)

D — $H\cdots A$	<i>D</i> —H	$H\cdots A$	$D \cdots A$	<i>D</i> —H··· <i>A</i>
C2—H2B···Se1 ⁱ	0.99	2.93	3.850 (4)	155
C5—H5A···I1 ⁱⁱ	0.99	3.30	4.150 (4)	145

Symmetry codes: (i) x, y, z+1; (ii) -x+1, -y+1, -z+1.

Table 22 Hydrogen-bond geometry (Å, °) for (2SDiazMesS_14F4DIB_t)

D — $H \cdots A$	<i>D</i> —H	$H\cdots A$	$D \cdots A$	D — $H \cdots A$
C2—H2 <i>B</i> ····S1 ⁱ	0.99	2.88	3.609 (3)	131

Symmetry code: (i) x+1, y, z.

Table 23 Hydrogen-bond geometry (Å, °) for (2SDiazMesSe_14F4DIB_t)

D — $H \cdots A$	<i>D</i> —H	$H\cdots A$	$D \cdots A$	<i>D</i> —H··· <i>A</i>
C2—H2B····Se1 ⁱ	0.99	2.83	3.5653 (13)	132

Symmetry code: (i) x+1, y, z.

Table 24 Hydrogen-bond geometry (Å, °) for (2SDiazMesS_14F4DIB_m)

D— H ··· A	<i>D</i> —H	$H\cdots A$	$D \cdots A$	<i>D</i> —H··· <i>A</i>
C2—H2A···F2i	0.99	2.44	3.310 (2)	146
C2—H2 <i>B</i> ···S1 ⁱⁱ	0.99	2.91	3.898 (2)	173

Symmetry codes: (i) x-1, y, z; (ii) x, -y+3/2, z+1/2.

Table 25 Hydrogen-bond geometry (Å, °) for (SDiazMesS 135F3I3B)

D— H ··· A	<i>D</i> —H	$H\cdots A$	$D \cdots A$	D — $H \cdots A$
C2—H2 <i>A</i> ···I6 ⁱ	0.99	3.30	4.234 (9)	158
C4—H4 <i>A</i> ····S1 ⁱⁱ	0.99	2.88	3.548 (10)	125
C5—H5 <i>B</i> ····F6 ⁱ	0.99	2.58	3.365 (11)	136
C25—H25 <i>B</i> ···I5 ⁱⁱⁱ	0.99	3.12	3.960 (13)	144
C26—H26 <i>B</i> ···I7 ⁱⁱⁱ	0.99	3.13	3.854 (11)	131
C27—H27 <i>B</i> ····F3 ^{iv}	0.99	2.48	3.283 (11)	138
C25 <i>B</i> —H25 <i>C</i> ···I7 ⁱⁱⁱ	0.99	3.24	4.06 (3)	141
C26 <i>B</i> —H26 <i>D</i> ···S2 ⁱⁱⁱ	0.99	2.85	3.60 (3)	134
C50—H50 <i>A</i> ···I9 ^v	0.99	3.07	3.843 (9)	136
C51—H51 <i>B</i> ···I3	0.99	3.13	4.083 (9)	162

Symmetry codes: (i) -x, y+1/2, -z+1/2; (ii) x, y+1, z; (iii) x, y-1, z; (iv) x, -y+1/2, z+1/2; (v) -x+1, -y+1, -z+1.

Table 26 Hydrogen-bond geometry (Å, °) for (SDiazMesSe 135F3I3B)

D — $H\cdots A$	<i>D</i> —H	$H\cdots A$	$D \cdots A$	<i>D</i> —H··· <i>A</i>
C4—H4 <i>A</i> ···I2 ⁱ	0.99	3.17	3.899 (4)	132
C4—H4A···Se1 ⁱⁱ	0.99	3.04	3.771 (4)	132
C5—H5 <i>B</i> ···I1	0.99	3.08	4.051 (4)	167

Symmetry codes: (i) x, y, z+1; (ii) x-1, y, z.

Table 27 Hydrogen-bond geometry (Å, °) for (2SDiazMesSe_5F5IB)

D— $H \cdots A$ D—H $H \cdots A$ $D \cdots A$ D— $H \cdots A$

C2—H2 <i>A</i> ···I2 ⁱ	0.99	3.25	3.852 (3)	121
C3—H3 <i>B</i> ····F12 ⁱ	0.99	2.54	3.456 (4)	155
C5—H5 <i>B</i> ····F4 ⁱⁱ	0.99	2.55	3.530 (3)	170

Symmetry codes: (i) x, -y+1/2, z-1/2; (ii) -x+1, y+1/2, -z+1/2.

Table 28 Hydrogen-bond geometry (Å, °) for (2SDiazMesS TIE)

D— H ··· A	<i>D</i> —H	$\mathbf{H}\cdots A$	$D \cdots A$	<i>D</i> —H··· <i>A</i>
C4 <i>B</i> —H4 <i>BB</i> ···S1 ⁱ	0.99	2.97	3.72 (3)	133

Symmetry code: (i) x–1, y, z.

Table 29 Hydrogen-bond geometry (Å, °) for (2SDiazMesSe TIE)

D — $H \cdots A$	<i>D</i> —H	$H\cdots A$	$D \cdots A$	D — $H \cdots A$
C4A—H4AB···Se1 ⁱ	0.99	2.97	3.73 (3)	134

Symmetry code: (i) x-1, y, z.

References

Aakeroy, C. B., Bryce, D. L., Desiraju, G. R., Frontera, A., Legon, A. C., Nicotra, F., Rissanen, K., Scheiner, S., Terraneo, G., Metrangolo, P. & Resnati, G. (2019). *Pure Appl. Chem.* **91**, 1889–1892.

Arman, H. D., Gieseking, R. L., Hanks, T. W. & Pennington, W. T. (2010). *Chem. Commun.* 46, 1854–1856.

Bruker (2017). APEX3, SADABS, and SAINT. Bruker AXS Inc., Madison, Wisconsin, USA.

Chernysheva, M. V. & Haukka, M. (2021). J. Solid State Chem. 293, 121759.

Chernysheva, M. V., Rautiainen, J. M., Ding, X. & Haukka, M. (2021). J. Solid State Chem. 295,.

Desiraju, G. R., Shing Ho, P., Kloo, L., Legon, A. C., Marquardt, R., Metrangolo, P., Politzer, P., Resnati, G. & Rissanen, K. (2013). *Pure Appl. Chem.* **85**, 1711–1713.

Dolomanov, O. V., Bourhis, L. J., Gildea, R. J., Howard, J. A. K. & Puschmann, H. (2009). *J. Appl. Crystallogr.* **42**, 339–341.

Groom, C. R., Bruno, I. J., Lightfoot, M. P. & Ward, S. C. (2016). *Acta Crystallogr. Sect. B Struct. Sci. Cryst. Eng. Mater.* **72**, 171–179.

- Iglesias, M., Beetstra, D. J., Knight, J. C., Ooi, L. L., Stasch, A., Coles, S., Male, L., Hursthouse, M. B., Cavell, K. J., Dervisi, A. & Fallis, I. A. (2008). *Organometallics*. 27, 3279–3289.
- Juárez-Pérez, E. J., Aragoni, M. C., Arca, M., Blake, A. J., Devillanova, F. A., Garau, A., Isaia, F., Lippolis, V., Núñez, R., Pintus, A. & Wilson, C. (2011). *Chem. A Eur. J.* 17, 11497–11514.
- Kobra, K., O'Donnell, S., Ferrari, A., McMillen, C. D. & Pennington, W. T. (2018). *New J. Chem.* 42, 10518–10528.
- Kuhn, K. M. & Grubbs, R. H. (2008). Org. Lett. 10, 2075–2077.
- Murray, J. S., Lane, P. & Politzer, P. (2009). J. Mol. Model. 15, 723–729.
- Pauling, L. (1960). The Nature of the Chemical Bond Ithaca, NY: Cornell University Press.
- Peloquin, A. J., Alapati, S., McMillen, C. D., Hanks, T. W. & Pennington, W. T. (2021). *Molecules*. **26**, 4985–4994.
- Peloquin, A. J., McCollum, J. M., McMillen, C. D. & Pennington, W. T. (2021). *Angew. Chemie Int. Ed.* **80918**, 22983–22989.
- Peloquin, A. J., McMillen, C. D., Iacono, S. T. & Pennington, W. T. (2021a). *Chempluschem.* **86**, 549–557.
- Peloquin, A., McMillen, C. D., Iacono, S. T. & Pennington, W. T. (2021b). *Chem. A Eur. J.* **27**, 8398–8405.
- Politzer, P. & Murray, J. S. (2017). Crystals. 7, 212–226.
- Politzer, P., Murray, J. S. & Clark, T. (2010). Phys. Chem. Chem. Phys. 12, 7748–7757.
- Rais, E., Flörke, U. & Wilhelm, R. (2016). Zeitschrift Fur Naturforsch. Sect. B J. Chem. Sci. 71, 667–676.
- Sheldrick, G. M. (2015a). Acta Crystallogr. Sect. C Struct. Chem. 71, 3–8.
- Sheldrick, G. M. (2015b). Acta Crystallogr. Sect. A Found. Crystallogr. 71, 3–8.
- Tomkowiak, H. & Katrusiak, A. (2018). J. Phys. Chem. C. 122, 5064–5070.
- Topić, F. & Rissanen, K. (2016). J. Am. Chem. Soc. 138, 6610-6616.
- Vogel, L., Wonner, P. & Huber, S. M. (2019). Angew. Chemie Int. Ed. 58, 1880-1891.

Supporting information